In situ formation and spatial variability of particle number concentration in a European Megacity

Michael Pikridas[1,2,3], Jean Sciare[4,3], Friederike Freutel[5], Suzanne Crumeyrolle[6*], Sarah-Lena von der Weiden-Reinmüller[5], Agnes Borbon[7], Alfons Schwarzenboeck[6], Maik Merkel[8], Monica Crippa[9], Evangelia Kostenidou[1,2], Magda Psichoudaki[1,2], Lea Hildebrandt[10], Gabriella J. Engelhart[10], Tuukka Petäjä[11], Andre S. H. Prévôt[9], Frank Drewnick[5], Urs Baltensperger[9], Alfred Wiedensohler[8], Markku Kulmala[11], Matthias Beekmann[7], and Spyros N. Pandis[1,2,10]

[1]Department of Chemical Engineering, University of Patras, Greece
[2]Institute of Chemical Engineering Sciences (ICEHT), FORTH, Patras, Greece
[3]The Cyprus Institute, Environment Energy and Water Resources Center, Nicosia, Cyprus
[4]Laboratoire des Sciences du Climat et de l'Environnement (LSCE), Gif/Yvette, France
[5]Max Planck Institute for Chemistry, Particle Chemistry Department, Mainz, Germany
[6]Laboratoire Meteorologie Physique (LaMP), 24 avenue des Landais, 63177, Aubiere, France
[7]Laboratoire Interuniversitaire des Systemes Atmospheriques, CNRS, Universites Paris-Est & Paris Diderot, 61 av. Du Gal de Gaulle, 94010 Creteil, France
[8]Leibniz Institute for Tropospheric Research, Leipzig, Germany
[9]Paul Scherrer Institute, Laboratory of Atmospheric Chemistry, Villigen, Switzerland
[10]Department of Chemical Engineering, Carnegie Mellon University, Pittsburgh, USA
[11]Department of Physics, University of Helsinki, Helsinki, Finland

* now at LOA, UMR8518, CNRS – Université Lille1, Villeneuve d'Ascq, France

Abstract

Ambient particle number size distributions were measured in Paris, France during summer (1 - 31 July 2009) and winter (15 January – 15 February 2010) at three fixed ground sites and using two mobile laboratories and one airplane. The campaigns were part of the MEGAPOLI project. New particle formation (NPF) was observed only during summer at approximately 50% of the campaign days, assisted by the low condensation sink (about $10.7\pm5.9\times10^{-3}$ s^{-1}). NPF events inside the Paris plume were also observed at 600 m altitude onboard an aircraft simultaneously with regional events identified on the ground. Increased particle number concentrations were measured aloft also outside of the Paris plume at the same altitude, and were attributed to NPF. The Paris plume was identified, based on increased particle number and black carbon concentration, up to 200 km away from Paris center during summer. The number concentration of particles with diameter

exceeding 2.5 nm measured on the surface at Paris center was on average $6.9\pm8.7\times10^4$ cm^{-3} and $12.1\pm8.6\times10^4$ cm^{-3} during summer and winter, respectively, and was found to decrease exponentially with distance from Paris. However, further than 30 km from the city center, the particle number concentration at the surface was similar during both campaigns. During summer one suburban site in the NE was not significantly affected by Paris emissions due to higher background number concentrations, while the particle number concentration at the second suburban site in the SW increased by a factor of three when it was downwind of Paris.

1. Introduction

Urban areas in the developed and developing world have been growing annually by 0.7% in population since 2005 and comprised approximately 54% of the total population of the planet in 2014 (United Nations, 2014). In this work, following the definition of the Organization for Economic Co-operation and Development (OECD), urban areas are defined as corresponding to a population density greater than 1500 inhabitants per km^2 (OECD, 2013). Several of these urban areas have increased in size to mega-centers, attracting more than 10 million inhabitants. This has led to an increasing demand for transportation, energy and industrial activity, which resulted in concentrated emission of gases and particulate matter (PM) impacting local air quality (Molina and Molina, 2004; Molina et al., 2004; Lawrence et al., 2007; Gurjar et al., 2008). Several epidemiological studies suggest that the risk of cancer, particularly lung cancer, is increased for people residing in areas affected by urban air pollution (Barbone et al., 1995; Beeson et al., 1998; Laden et al., 2006; Nyberg et al., 2000; Pope et al., 2002; Nafstad et al., 2003). Pope et al. (2009) and Wang et al. (2008) showed that fine particles with diameter smaller than 2.5 µm ($PM_{2.5}$) are related to increased mortality.

Aerosol particles can change climate patterns and the hydrological cycle on regional and global scales (Chung et al., 2005; Lohmann and Feichter, 2005; IPCC, 2007). Submicrometer particles, down to 100 nm, are the most effective ones in scattering solar radiation. The uncertainties in the primary emission rates of these pollutants and in their formation from gaseous precursors are still large. On a global scale new particle formation (NPF), that is nucleation of low volatility vapors and subsequent condensational growth to larger sizes, is the major reason for high particle number concentrations (Kulmala et al., 2004). The mechanism behind this major particle formation process is still not completely understood (Riccobono et al., 2014). This uncertainty has a direct impact on our understanding of the role of nucleated particles in climate change (Pierce and Adams, 2009). NPF is often a regional phenomenon covering areas of several hundred square kilometers (Vana et al., 2004; Stanier et al., 2004a; Komppula et al., 2006; Crumeyrolle et al., 2010) but it can be space-restricted when the source of one of the nucleating vapors is space limited, as it has been observed in coastal sites (Wen et al., 2006).

During the past decade a number of studies reported ambient particle number concentrations in urban areas. The measurement period spanned from a few months (Hering et al., 2007; Wang et al., 2010; Dunn et al., 2004; Baltensperger et al., 2002; McMurry et al., 2005), to one or more years (Woo et al., 2001; Alam et al., 2003; Shi, 2003; Wehner and Wiedensohler, 2003; Stanier et al., 2004b; Wehner et al., 2004; Wu et al., 2007; Rodriguez et al., 2005; Watson et al., 2006; Wåhlin, 2009). The majority of studies are based on observations from one or at most two stationary sites, assuming that these stations are representative of the area under investigation. Most of these studies have found higher concentrations during winter due to both increased emissions caused by higher energy demand, and lower boundary layer height. Also, typically a diurnal pattern has been found that shows peaks due to morning rush hour traffic during weekdays but not on weekends.

NPF has often been observed in urban areas (Woo et al., 2001; Baltensperger et al., 2002; Laakso et al., 2003; Tuch et al., 2003; Stanier et al., 2004a; Watson et al., 2006; Wu et al., 2007), but growth and nucleation rates are rarely reported in these studies (Birmili and Wiedensohler, 2000; McMurry, 2000; Shi et al., 2007; Wehner et al., 2007; Manninen et al., 2010).

During the "Megacities: Emissions, urban, regional and Global Atmospheric POLlution and climate effects, and Integrated tools for assessment and mitigation" (MEGAPOLI) project (Baklanov et al., 2010), measurements were conducted in and around the megacity of Paris. Gas and particulate phase measurements from three fixed ground sites, two mobile laboratories, and one airplane were collected for both summer 2009 and winter 2010. The residence time of the air mass over land was found to influence PM levels, with longer residence times leading to higher mass concentrations (Freutel et al., 2013). Air masses from the Atlantic, which were dominating during the summer campaign, led to relatively clean conditions (Freutel et al., 2013; Freney et al., 2014). Cooking was identified as a significant local organic aerosol source within Paris during summer with vehicular traffic being second (Crippa et al., 2013b). During winter residential wood burning was found to be a major source of organic aerosol (Crippa et al., 2013a). During both MEGAPOLI campaigns, the contribution of primary transportation emissions to submicrometer organic aerosol (OA) was around 6% (Crippa et al., 2013b). In the year of the MEGAPOLI campaigns, 61% of the light duty vehicles in France were powered by diesel engines and 72% of the consumed fuel was diesel (World Bank, 2012). The sulfur content of diesel in France at that time was 10 ppm compared for example to 500 ppm in 1998. The sulfur content of fuel affects both the total particle emissions but also the shape of the corresponding aerosol distribution (Platt et al., 2013; Bermúdez et al., 2015).

Beekmann et al. (2015) have presented a synthesis of the MEGAPOLI PM mass source attribution efforts based on the corresponding field measurements. In parallel, several modeling efforts have been also conducted examining the contribution of regional sources to fine PM (Skyllakou et al., 2014) and investigating the organic aerosol sources in Paris (Couvidat et al., 2013; Zhang et al., 2013). All of these studies focused on PM mass concentration and not on particle number. The different size distributions of the aerosol emitted by different sources usually result in very different source contributions to particle number and mass (Zhou et al., 2004). There have been a number of studies that tried to quantify the particle number sources using available size distribution measurements (Wåhlin et al., 2001; Hussein et al., 2004; Zhou et al., 2004; Chan and Mozurkewich, 2007). However, the changes of these distributions due to new particle formation and growth or other dynamic changes seriously limit the applicability of techniques like Positive Matrix Factorization (PMF). Zhou et al. (2004) excluded the corresponding new particle formation periods from their dataset to overcome this problem.

In this work we focus on the particle number concentrations in Paris and its surroundings during both (summer and winter) campaigns. The effect of the Paris megacity on the downwind areas is assessed together with the spatial extent of its influence. The frequency and spatial characteristics of new particle formation events are also investigated.

2. Sampling sites

Month long campaigns were conducted in the Parisian region during summer (1 July to 31 July 2009) and winter (15 January to 15 February 2010). They included monitoring of the aerosol size distribution along with composition, coupled with gas phase and meteorological monitoring.

The city of Paris is an urbanized area covering about 3000 km^2 with 2.2 million inhabitants. The greater Paris area, called Île de France (IDF), is one of the largest metropolitan areas in Europe including more than 12 million inhabitants. The administrative boundaries of Paris and IDF are shown in Fig. 1 along with the population density map of the area.

Detailed aerosol particle measurements were conducted at an urban and two sub-urban sites (Fig. 1). The Site Instrumental de Recherche par Télédétection Atmosphérique (SIRTA, 48° 43' 5" N and 2° 12' 26" E) is located on the campus of Ecole Polytechnique (Palaiseau), 20 km southwest of Paris center in a semi-urban environment inside the campus of Ecole Polytechnique. This site is surrounded by highways at 3-6 km distance in all wind directions. Measurements in the Laboratoire d'Hygiène de la Ville de Paris (LHVP, 48° 49' 11" N and 2° 21' 35'' E), inside of Paris, were performed on a terraced roof 14 m above ground level and on the ground inside a research container. This site includes a station of the AIRPARIF air quality monitoring network and is representative of the Paris urban background air pollution (Sciare et al., 2010; Favez et al., 2007). Finally the sub-urban station at Golf de la Poudrerie (GOLF, 48° 56' 2'' N and 2° 32' 49'' E**)** was located 20 km northeast of Paris center near a golf course and a forested park.

Two mobile platforms, named "MoLa" (Mobile Laboratory) and "MOSQUITA" (Measurements Of Spatial QUantitative Immissions of Trace gases and Aerosols), were operated by the Max Planck Institute for Chemistry (Drewnick et al., 2012; von der Weiden-Reinmüller et al., 2014a) and the Paul Scherrer Institute (Bukowiecki et al., 2002; Weimer et al., 2009), respectively. The measurement path of both mobile platforms was decided based on forecasts of the chemical transport model CHIMERE (Rouil et al., 2009; Menut and Bessagnet, 2010; Menut et al., 2013). Three measurement strategies were employed during both campaigns: stationary, axial and cross sectional measurements (von der Weiden-Reinmüller et al., 2014a; 2014b). Cross sectional (mobile) measurements were carried out by maintaining approximately constant distance from Paris center while varying the cardinal directions, allowing distinction between background concentrations and Paris emissions. Axial (mobile) measurements were conducted by maintaining approximately the same cardinal direction while varying the distance with respect to Paris center, thus monitoring the evolution of the plume. Stationary measurements were conducted when the direction of the Paris emissions, based on the CHIMERE model, were not stable enough to allow cross sectional or axial measurements. Stationary measurements were conducted only by MoLa either downwind of Paris, or upwind to assess background aerosol loadings.

The airborne measurements were performed by an ATR-42 and a Piper Aztec aircraft during summer and winter, respectively, operated by the French Service des Avions Français Instrumentés pour la Recherche en Environnement (SAFIRE). Each flight included a circle around IDF followed by crossing the expected Paris plume multiple times, at a constant altitude of 600 and 500 m above sea level for the summer and winter campaigns, respectively. During July 1 the flight path was kept at a constant altitude of approximately 800 m. Flights were performed on 11 out of the 31 days of the summer campaign. Fig. 2 shows the flight patterns and sampling days of the ATR-42 during summer. Flight days were selected based on CHIMERE predictions. Higher PM concentration days were favored, thus the observed aerosol properties are expected to be biased toward more polluted conditions. During winter two flights per sampling day were conducted for four days (January 27 and 31, February 14 and 15). The first flight included a survey of the aerosol properties around IDF and the second monitored the Paris plume, following a flight path similar to the summer one.

2.1 Instrumentation

The MEGAPOLI project focused on the properties of ambient aerosol, including both mass and number concentration measurements. This work examines the particle number concentration N during both MEGAPOLI campaigns; the instruments and measurements relevant for this purpose are summarized in Table 1. A number of additional measurements of concentrations of gas-phase pollutants, radicals, etc., were conducted during the campaigns (Michoud et al., 2012), but are not used in the present work because they did not provide any additional insights.

At SIRTA, two instruments were used to monitor the ambient particle number distribution. A Scanning Mobility Particle Sizer (SMPS; TSI Model 3936) sampled aerosol particles from 10 to 500 nm in diameter through an inlet located approximately at 4 m above ground. The particles were actively dried using a Nafion dryer. A Differential Mobility Particle Sizer (DMPS, Aalto et al., 2001) also monitored ambient number size distributions ranging from 6 to 800 nm during summer. At LHVP, the sampling inlet was located 6 m above ground and the aerosol sample was dried using a diffusion dryer as described in Tuch et al. (2009) before entering a mobility particle size spectrometer

TROPOS-type TDMPS (Twin Differential Mobility Particle Sizer; Birmili et al., 1999), which monitored the aerosol size distribution from 3 to 630 nm. At the same site, an Air Ion Spectrometer (AIS; Mirme et al., 2007) monitored the size distribution of ambient (not dried) positive and negative air ions of mobility diameters ranging from 0.8 to 40 nm. To minimize particle losses the sampling line length of the AIS was 30 cm. At GOLF, the particle size distribution between 5 nm and 1 µm was monitored with an Electrical Aerosol Spectrometer (EAS, Airel Ltd.) and sampling was conducted 8 m above ground. Because the three aerosol size distribution instruments (SMPS, TDMPS, EAS) used for the stationary ground measurements during both campaigns overlap between 10 nm and 500 nm (mobility diameter), our analysis will focus on this size range, denoted as $N_{10\text{-}500}$.

MoLa, which was based at GOLF, monitored the total particle number concentration via an Ultrafine Water Condensation Particle Counter (UWCPC, TSI Model 3786) with 50% detection efficiency at 2.5 nm, which will be denoted as $N_{2.5}$. The aerosol inlet during stationary measurements was located at approximately the same height as the stationary measurements at GOLF (8 m above ground). During mobile measurements, sampling occurred at about 2.4 m above ground level. MOSQUITA monitored the total particle number concentration via a butanol-based Condensation Particle Counter (CPC; TSI Model 3010, 50% detection efficiency at 10 nm) during summer, further denoted as N_{10}, and via an Ultra High Sensitivity Aerosol Spectrometer (UHSAS; DMT Model A) during winter. The UHSAS monitored the size distribution, with respect to the optical diameter, ranging from 60 nm to 1 µm.

On-board the METEO-FRANCE aircraft (ATR-42), aerosols were sampled, under dry conditions, through the community aerosol inlet and delivered to a comprehensive suite of aerosol instruments. This isokinetic and isoaxial inlet is based on the University of Hawaii shrouded solid diffuser designed by A. Clarke and had been modified by Meteo France (McNaughton et al., 2007). Particle number concentration was monitored directly during summer and winter flights using a CPC with 10 nm (TSI Model 3010) and 2.5 nm (TSI Model 3025) lower cutoff, respectively. Because the CPCs used during the summer and winter campaigns had different lower detection limits, the corresponding number concentrations will be denoted as N_{10} and $N_{2.5}$, respectively.

In order to quantify potential differences between instruments, at least one of the mobile laboratories visited each site for 5-15 hours during each campaign. During summer, the differences in number concentration between the CPC on board the visiting mobile laboratory (MOSQUITA) and the aerosol sizing instrument at each of the stationary sites did not exceed 10% (Figure S1 in the Supplementary Information). The CPC on board MOSQUITA had a detection size limit equal to approximately 10 nm. During winter the MoLa CPC, with a lower detection size limit of 2.5 nm, was employed for the intercomparisons. In this case, the differences were higher and equal to 30%, 18%, and 19% at SIRTA, LHVP, and GOLF, respectively. Taking into account that particles below 10 nm were typically present at SIRTA during winter the corresponding discrepancy can be partially explained by the different detection limits of the two instruments (10 nm for the SMPS at SIRTA and 2.5 nm for the MoLa CPC). During both campaigns the number concentrations monitored onboard MoLa and MOSQUITA were also compared for approximately 8 hours. The two instruments were found to agree when the concentrations of the nucleation mode particles were moderate or low. This is expected due to their different size detection limits. The results of this intercomparison have been presented by von der Weiden-Reinmüller et al. (2014a).

3. Methods

3.1 Particle formation event categorization

Particle formation events have been categorized in the past based on the concentration of 1.6 – 7.5 nm air ions (Hiirsiko et al., 2007; Vana et al., 2008) and on the concentration of total ambient particles below 25 nm (Stanier et al., 2004a; Dal Maso et al., 2005). At LHVP both air ions and ambient particles were measured and therefore we used two classification schemes, one based solely on ambient particles following Dal Maso et al. (2005) and one that includes air ions, following Hirsikko et al. (2007). In both cases, the observation period was divided into particle formation event days, non-event days and undefined days. In general, a day is classified as event day if a nucleation mode (particles with sizes smaller than 10 nm) is present for several hours and grows continuously during the course of the day. If no traces of a nucleation mode are seen, a day is classified as a non-event day. Days that did not clearly belong to either of the aforementioned categories were classified as undefined. Examples of event, undefined and non-event days are shown in Figs. 3, 4 and 5, respectively.

During July 12, a nucleation mode appeared at 14:00 LST (local standard time) simultaneously at all ground sites (Fig. 3). During this cloudy day, nucleation was observed approximately one hour after the solar intensity increased by a factor of three (from 300 to 1070 W m^{-2}). This day was consequently classified as event day. During July

10, an increase in the number concentration of particles above 10 nm in diameter was measured simultaneously at LHVP and SIRTA at 14:00 LST (Fig. 4). It was unclear whether the mode also appeared at GOLF due to interferences by local sources. Particle growth was not continuous and the mode disappeared abruptly after approximately three hours, even though the direction of the wind did not change at this time. At LHVP air ion bursts in the size range between 1.6 – 7.5 nm did not follow a distinct pattern but were random. As a result it was unclear whether NPF occurred and the day was classified as undefined for all sites. During July 29, no nucleation event was observed, and the day was consequently classified as non-event day. During this day, the condensation sink (CS) was rather high ($9.0\pm1.7\times10^{-3}$ s^{-1}, $20.3\pm9.7\times10^{-3}$ s^{-1} and $14.4\pm4.1\times10^{-3}$ s^{-1} at SIRTA, LHVP and GOLF respectively) from 08:00 to 16:00 LST, when NPF was expected to occur. These sink values were above the summer average for all sites (see Section 3.3) and contributed to the lack of a nucleation mode at all sites (Fig. 5).

3.2 Duration of nucleation events

The duration of nucleation events at LHVP was calculated based on AIS measurements following the procedure described by Hirsikko et al. (2005) and Pikridas et al. (2012). In brief, a normal distribution was fitted to the time series of concentration of air ions with diameters between 2 and 5 nm. The beginning of the event was determined by the initial increase of the air ion concentration (assuming a stable air ion concentration before the event) and the end by the peak of the normal distribution. A decrease of the number concentration implies that the rate of particle production is lower than the combined rates of coagulation and particle growth to diameters greater than 5 nm, or that the air mass is getting diluted; it does not necessarily imply that the rate of production is zero. Our calculated event-end is thus a lower bound estimate.

3.3 Condensation sink

The condensation sink (CS) is defined as the condensational loss rate constant of vapors (Kulmala et al., 2001; Dal Maso et al., 2002). The CS values were calculated using:

$$CS = 2\pi D \int_0^\infty D_p \beta_m(D_p) n(D_p) dD_p = 2\pi D \sum_i D_{pi} \beta_{mi} N_i \qquad (1)$$

where D is the diffusion coefficient of the condensing vapor, D_{pi} is the diameter and N_i the particle number concentration in size class. The term β_{mi} corresponds to the transition regime correction factor for the size class *i*, which was calculated based on Fuchs and Sutugin (1971). The properties of the condensable vapors are assumed to be similar to those of sulfuric acid, without accounting for hydration, leading to an upper limit estimate. If the aerosol sample was dried prior to the measurement, the diameter reduction due to water loss was estimated using the Extended Aerosol Inorganic Model II (E-AIM, http://www.aim.env.uea.ac.uk/aim/aim.php; Carslaw et al., 1995; Clegg et al., 1998; Massucci et al., 1999). The hourly averaged inorganic concentrations for sulfate, ammonium and nitrate measured by the aerosol mass spectrometer (AMS; Jayne et al., 2000; Jimenez et al., 2003) and ambient RH measured at each site, were used as inputs to the model, neglecting any contribution of organics to the aerosol water content. The volume growth factor was determined following the method of Engelhart et al. (2011) which assumes that all submicrometer particles grow similarly by neglecting the Kelvin effects. The diameter growth factor was calculated as the cubic root of the volume growth factor and was applied to the whole particle distribution.

3.4 Mobile measurements

Due to the high frequency of local contamination events, mobile data was post-processed by examining video footage recorded at the driver's cabin of the mobile laboratory, based on Drewnick et al. (2012). Measurement periods were omitted from analysis if traffic was identified less than 150 m from the platform; if human activities (e.g. cooking, heating) were spotted; when driving at low speed caused a possible contamination by the vehicle's own exhaust; and when travelling inside tunnels. In order to reduce the amount of contaminated data major roads were avoided. More details concerning the conditioning of mobile measurements presented in this study can be found in von der Weiden-Reinmüller et al. (2014a). Further analysis of the mobile dataset was conducted based on results from the particle dispersion model FLEXPART performed in forward mode (Stohl et al., 2005). Particles were released from an area whose borders were determined by the population density map presented on Fig. 1 and included Paris. Based on these modeling results and the respective measurement tracks, mobile measurements were attributed as influenced or not by Paris emissions.

4. Meteorology

During summer, the lowest ambient temperature was 12°C, observed at SIRTA and GOLF, and the highest of 33°C was measured at LHVP. Campaign average temperatures during summer were 19.7, 21.1 and 18.7 °C at GOLF, LHVP and SIRTA, respectively. In general, the temperature was higher inside the city center by 1°C at least, compared to the suburban sites. Diurnal variations of RH (ranging from 35% to 90%) and temperature were similar at all sites during summer. There were several cloudy periods and cloud coverage was geographically dependent. During summer at all ground sites, solar radiation reached a maximum of 900 W m^{-2} while the presence of clouds could reduce it by a factor of three. Precipitation as monitored at SIRTA occurred on 8 of the 31 days of the campaign (July 8, 16-18, 22, 23, 27 and 30). Maximum observed precipitation rate during the summer campaign was 0.5 mm min^{-1}; however it rarely exceeded 0.1 mm min^{-1}.

During winter the campaign average ambient temperatures were 2.6, 3.3 and 1.2 °C at GOLF, LHVP, and SIRTA, respectively. RH varied from 40% to 90% and exceeded 95% on several occasions at all sites. Hourly average global solar irradiance did not exceed 400 W m^{-2} during the winter campaign and did not exceed 100 W m^{-2} on 14 of the 32 days of observations. Precipitation occurred during winter on two thirds (21 of 32 days) of the campaign days and the average precipitation rate was approximately 0.15 mm min^{-1} .

Figure 6 shows the wind direction distribution at all sites, for each campaign. Wind direction, measured at 10 m above ground, during summer was predominantly SW at LHVP and GOLF and W at SIRTA (Fig. 6) indicating that air masses often crossed the city center before reaching GOLF and that SIRTA was mostly upwind of the city. During winter wind directions were more variable with the wind equally coming from both NE and W (Fig 6). During the winter campaign SIRTA was more often than GOLF influenced by air masses that crossed the urban area before reaching the site.

5 Particle number concentrations and size distributions

5.1 Stationary measurements

Average number concentrations of particles with diameters between 10 and 500 nm (N_{10-500}), for all ground sites during both campaigns, are summarized in Table 2. On average, the N_{10-500} concentrations during winter were higher than during summer by a factor of two at SIRTA and GOLF, and by 35% at LHVP. The highest hourly averaged concentrations were observed at GOLF (54.1×10^3 cm^{-3} and 72.2×10^3 cm^{-3} during summer and winter, respectively) followed by the urban center station LHVP (34.4×10^3 cm^{-3} and 45.5×10^3 cm^{-3} during summer and winter, respectively). The average ratio of the aerosol number concentration observed at LHVP to the one observed at GOLF was 0.86 and 0.62 during summer and winter, respectively. The average ratio of the aerosol number concentration observed at LHVP to the one observed at SIRTA was 2.1 and 1.5 during summer and winter, respectively.

The particle number concentration at all sites followed the same diurnal pattern during both seasons (Fig. 7). Regardless of site and season, minimum concentrations were observed between 3:00 and 4:00 LST, when anthropogenic activities are expected to be minimal. The concentration exhibited two maxima: during morning traffic hours, peaking between 7:00 and 10:00 LST, and during nighttime, between 8:00 and 9:00 LST. These diurnal profiles are typical of urban areas (Ruuskanen et al., 2001; Woo et al., 2001; Watson et al., 2006).) and can be explained based on the evolution of the mixing layer (Bukowiecki et al., 2005). In the afternoon atmospheric mixing reaches its maximum and primary pollutant concentrations decrease due to dilution. The mixing height remains fairly constant till nighttime when it decreases resulting in increasing primary pollutant levels. Boundary layer measurements using a Cloud and Aerosol Micro Lidar (Cimel model CE-370) at 355 nm that were performed at SIRTA support this explanation. The magnitude and time of the peaks varied depending on site and season. By comparing these maxima, which correspond to the peak of anthropogenic activity, against the minimum of the diurnal cycle, a rough estimate of the $N_{10\text{-}500}$ anthropogenic contribution can be made for each site. During summer the increase was 84%, 79%, and 21% at GOLF, LHVP, and SIRTA respectively, and during winter and 153%, 133% and 141%.

During summer, particles with diameter ranging from 30 to 100 nm dominated the $N_{10\text{-}500}$ at SIRTA, accounting on average for 53%, followed by particles with diameters ranging from 10 to 30 nm which accounted for 30% (Fig. 8). Similar behavior was observed at LHVP during summer, where particles with diameter ranging from 30 to 100 nm accounted for 47% and particles with diameters ranging from 10 to 30 nm for 40% of the $N_{10\text{-}500}$. However, $N_{10\text{-}500}$ measured at GOLF was dominated by particles with diameter ranging from 10 to 30 nm, which accounted for 50% of the $N_{10\text{-}500}$, followed by particles with diameter ranging from 30 to 100 nm that accounted for 42%.

Average size distributions for each site are shown in Fig. 8, along with the corresponding lognormal modes. During summer, an Aitken mode centered approximately at 35 nm was dominating the number distributions at LHVP and SIRTA. Nucleated particles grew to approximately this size during summer (see Fig. 3 and 4) and could be identified for several hours after each event. The average number size distribution in LHVP and SIRTA usually had two more modes centered at 15 and 115 nm respectively. The summertime number distribution at GOLF was characterized by two modes centered at approximately 15 and 80 nm. Unlike SIRTA and LHVP the 15 nm mode dominated the aerosol number distribution at GOLF.

During winter the contribution of particles with diameter from 10 to 30 nm to $N_{10\text{-}500}$ was almost equal to that from particles with diameters 30 to 100 nm at SIRTA (42% and 39%, respectively) and LHVP (44% and 40%, respectively). At GOLF the contribution of particles with diameters between 10 to 30 nm increased even further (compared to summer) reaching 56%, and the contribution of particles with diameters between 30 and 100 nm decreased to 34%. The average size distribution, shown in Fig. 8, indicates a dominating mode centered below 20 nm at all sites and a smaller second mode at 60, 80, and 50 nm at SIRTA, LHVP and GOLF, respectively. Similar shifts of the aerosol distribution to lower sizes during winter has been observed elsewhere (Bukowiecki et al., 2003) where an inverse temperature dependence of the particle number concentration was reported. Particles larger than 100 nm accounted for less than 20% of $N_{10\text{-}500}$ during both campaigns at all sites.

Taking into account the location of each site, the contribution of small particles (diameters 10-30 nm) to $N_{10\text{-}500}$ increases when moving from the SW (SIRTA) to the NE of Paris (GOLF). Consequently, the contribution of particles with sizes 30-100 nm to the $N_{10\text{-}500}$ exhibits a decreasing (opposite) trend from the SW to the NE of Paris. Both trends were observed during both seasons and indicate a persistent source of particles with diameters smaller than 30 nm NE of Paris, where GOLF was located. This conclusion is further supported by mobile measurements (Section 5.3) that showed that the background $N_{2.5}$ was relatively stable in the area further than GOLF during summer.

5.2 Impact of Paris on its surroundings

To investigate the impact of the emissions from the city center on number concentrations at the two satellite sites (GOLF, LHVP) the measurements were separated with respect to wind direction, excluding periods when the wind speed was below 1 m s^{-1} (Fig. 9). Taking into account that the area is relatively flat, it was assumed that the urban center influences each of the satellite sites at certain wind directions (215±30º and 65±30º for GOLF and SIRTA, respectively), noted with red on Fig. 9. This analysis is complicated by the variability in aerosol load due to air mass origin difference. During most of the summer campaign clean air masses from the Atlantic were reaching Paris (Freutel et al., 2013). Air masses of different origin, which accounted for only two consequent days during the summer campaign were omitted to minimize any discrepancy. During winter air mass origin was more variable and a common background could not be ensured, limiting this analysis only to the summer campaign.

During summer, the highest N_{10-500} measured at SIRTA was observed when the air masses crossed the city center (9.8±3.5×10^3 cm^{-3} and the lowest when the wind originated from the opposite direction (4.2±2.3×10^3 cm^{-3}) considered later on as the background concentration. The urban emissions led thus to an increase of the number concentration by a factor of two at SIRTA. On the contrary, at GOLF the N_{10-500} was not clearly affected by the wind direction during July 2009. N_{10-500} measurements at GOLF were higher than at SIRTA, located at the same distance from Paris but on the opposite direction, by a factor of three when either site was not influenced by Paris. These results do not imply that Paris did not affect its surroundings during summer, but rather that the effect of the city was not large enough to be observed due to higher background concentrations at the GOLF site in the NE of Paris with respect to those at the SIRTA site in the SW. Mobile measurements that covered mainly the N-NE area with respect to Paris support this result (see Section 5.3). The possibility that these observations were due to temperature changes (Bukowiecki et al., 2003) was also investigated. However, no clear dependence between temperature and N_{10-500} was established. As an example, at SIRTA the lowest temperatures (around 17 °C on average) were observed both when air masses were influenced by Paris and when the wind came from the opposite direction.

On July 21, MoLa performed stationary measurements 38 km north of Paris, which is almost twice the distance of each of the stationary sites (20 km) from the city center. Initially, air masses reaching MoLa were influenced by Paris emissions, based on FLEXPART simulations, and $N_{2.5}$ was equal to 14.1×10^3 cm^{-3}. However, the wind direction shifted while sampling and the $N_{2.5}$ decreased by 40% reaching approximately 8.5×10^3 cm^{-3}.

5.3 Spatial evolution of particle numbers in Paris and its surroundings

The majority of mobile measurements were conducted downwind of Paris in order to characterize its effect on its surroundings (von der Weiden-Reinmüller et al., 2014a; 2014b). These measurements were conducted in different distances from the center of Paris, under various meteorological conditions, different air mass origin (marine, continental) and were affected by the diurnal pattern (Fig. 7) of Paris emissions. The mobile measurements were further affected by wind direction shifts which resulted in monitoring of background concentrations instead of Paris emissions.

Paris emission measurements were identified during data analysis using FLEXPART in forward mode (Section 3.4). During summer, marine air masses were predominantly resulting in a relatively stable and low PM background. During winter air mass origin was not as stable as during summer, yet Paris emissions were also higher, thus facilitating the analysis. Variations in the number concentration due to meteorology effects or Paris emissions fluctuations can be dealt with by examining short case-study periods when these variables are relatively stable. However because such periods span a few hours only, the measurement sample is small. If measurements throughout each campaign are considered the sample size is satisfactory, yet it reflects the different conditions mentioned above. In this work both approaches were considered and are presented to quantify the behavior of the Paris plume downwind of the city.

Mobile measurements were separated, based on location, into concentric rings with borders at 0.15, 0.25, 0.4, 0.6, 0.8 and 1° (16.7, 27.8, 44.4, 66.7, 88.9, and 111.1 km) radius centered at kilometer zero of Paris (the official Paris center) as shown in Fig. 1. The first ring includes Paris and highly populated areas surrounding it, while the second one includes the greater Paris area where the two stationary sites (GOLF, SIRTA) are located.

During summer, when SW winds were predominant, the majority of the mobile measurements took place N-NE of Paris. The $N_{2.5}$ decreased exponentially with distance reaching $1.3 \pm 1.6 \times 10^4$ cm^{-3} approximately 100 km away from Paris center (Fig. 10), which is not statistically different at the 95% confidence interval from the average background (not influenced by Paris emissions) concentration ($1.4 \pm 1.6 \times 10^4$ cm^{-3}) measured during summer upwind at distances greater than 30 km from the city center by MoLa. However, at distances shorter than 30 km, where GOLF is located, the background $N_{2.5}$ was almost twice as large ($2.5 \pm 1.1 \times 10^4$ cm^{-3}) indicating a significant regional number source affecting this area. During 13 July 2009, axial measurements with respect to Paris were performed under relatively stable meteorological conditions and the results, shown as black dots in Fig. 10, are in good agreement with the campaign average values, following the same exponential decrease. Similar behavior in that area was observed for other pollutants during the same period (von der Weiden-Reinmüller et al., 2014b).

During winter, $N_{2.5}$ exhibited an exponential decrease with increasing distance from Paris center similar to summer. However, at the center $N_{2.5}$ was 75% higher than during summer. This difference was diminished in the Paris suburbs (second bar in Fig. 10), reaching 20%. At distances greater than 30 km from the Paris center, no statistical difference at the 95% confidence interval between $N_{2.5}$ measured during summer and winter was observed. Measured $N_{2.5}$ further than 70 km away from Paris remained stable (≈1.4±1.9×10^4) and was not statistically different from the background $N_{2.5}$ concentrations measured during winter (1.1±1.4×10^4 cm^{-3}) or summer (1.4±1.6×10^4 cm^{-3}). During 19 January 2010, axial measurements were performed and the results (shown as green triangles in Fig. 10) are also in good agreement with the winter campaign averages.

6. New particle formation at ground level

A summary of the particle formation categorization for both campaigns can be found in Fig. 11. During the summer campaign air ion bursts (of both polarities) for particles of sizes between 2 and5 nm were picked up by the AIS at LHVP on a daily basis (Fig. 11) with the exception of July 29. Concentrations of negatively charged particles between 2 and 10 nm were higher by one order of magnitude compared to positively charged. In Fig. 11 we present the NPF categorization based on the negative ions which provided a more sensitive way of identifying nucleation events.

During the summer campaign we observed 14 events at SIRTA, 14 at LHVP and 7 at GOLF based on SMPS, DMPS and EAS measurements, respectively. When NPF was identified at SIRTA it also took place at the city center (Fig. 11) with one exception (July 7). Due to technical issues of the DMPS, data for five days are not available at the LHVP site. Nucleation events, if identified at two or more of the ground sites, always occurred practically simultaneously (<10 min difference). $N_{10\text{-}500}$ typically doubled at GOLF due to NPF. At LHVP, an increase of $N_{10\text{-}500}$ ranging between 50% and 150% was observed due to NPF. The greatest increase in $N_{10\text{-}500}$, often exceeding 100%, due to NPF was observed at SIRTA.

The highest particle growth rate (17.6 nm h^{-1}), based on SMPS measurements, was observed at SIRTA on July 4 during a regional event observed at all ground sites while the lowest growth rate (1.6 nm h^{-1}) was observed on July 15 at LHVP, where typically lower daily growth rates compared to the two satellite sites were observed. The average growth rates were 6.1 ± 1.8 nm h^{-1}, 4.6±1.9 nm h^{-1} and 5.5±4.1 nm h^{-1}, at GOLF, LHVP and SIRTA, respectively, during the summer campaign (Table 2). Growth rates for events that occurred on all sites on the same day were 5.9± 2.4 nm h^{-1}, 4.5±2.0 nm h^{-1} and 8.3±5.6 nm h^{-1}, at GOLF, LHVP and SIRTA, respectively.

During July 28 nocturnal particle formation was observed at LHVP, which was identified by an increase of the ion number concentration within the 1.2–1.7 nm size range.

An apparent growth of cluster ions to larger diameters than the upper limit of the preexisting ion pool was evident but air ions did not grow above 2 nm. Nocturnal cluster growth has been observed in remote areas (Junninen et al., 2008; Kalivitis et al., 2012; Hirsikko et al., 2012) and has been linked to the presence of monoterpenes (Ortega et al., 2012). Sulfuric acid generation due to nighttime oxidation processes has also been observed before (Mauldin et al., 2003).

The CS during the summer campaign for all sites is shown in Fig. S2 of the Supplementary Information, where event and undefined days are marked with blue and light blue labels, respectively. During summer the CS was half the value than in winter at GOLF ($11.7\pm11.6\times10^{-3}s^{-1}$ in summer compared to $21.5\pm14.4\times10^{-3}s^{-1}$ in winter) and SIRTA ($5.7\pm3.5\times10^{-3}s^{-1}$ compared to $12.3\pm6.8\times10^{-3}s^{-1}$) and 30% lower at LHVP ($12.8\pm7.5\times10^{-3}s^{-1}$ compared to $17.0\pm8.6\times10^{-3}s^{-1}$). During summer at SIRTA and LHVP, NPF events occurred when the CS was lower than the seasonal average by 45% and 25%, respectively. Undefined events at both sites were associated with CS similar to the seasonal average value and non-event days with 25-30% higher CS compared to the seasonal average. In winter, the high CS values in conjunction with the low solar intensity (see Section 4) most likely prevented nanoparticle growth and resulted in only five events without significant growth, identified only by the AIS at LHVP.

The solar intensity influence on NPF event occurrence was evident at SIRTA and LHVP. During NPF events at these two sites solar intensity was on average 30% and 20% higher, respectively, compared to non-event days. At GOLF, solar intensity during non-event days was found to be higher by 8% compared to actual event periods.

At GOLF, seven NPF events were identified, corresponding to a monthly frequency of 23%. The event frequency difference between GOLF and the other two ground stations was partially due to a higher frequency (23%) of undefined days (Fig. 11) caused by interferences of nearby traffic. When no event was identified at all sites the CS at GOLF was double ($14.7\pm4.5\times10^{-3}$ s^{-1}) compared to event days ($7.3\pm0.8\times10^{-3}$ s^{-1}), indicating that, similarly to the other sites, the CS was contributing to the inhibition of NPF occurrence. On several occasions (July 2, 6, 8, 23, and 28), NPF events were identified at LHVP and SIRTA (on July 8 it was not clear if NPF at SIRTA occurred) but not at GOLF (Suppl. Fig. S3). During these days CS values at GOLF were similar to event days and lower by 30% compared to the campaign average, indicating that at least the CS was not suppressing NPF. On two occasions (July 6 and 8) the observations show a continuous mode below 30 nm, either due to electrometer noise or local interferences, which prevented identification of NPF. Both days were listed as non-event days but NPF may have occurred. During July 2, a nucleation mode was observed at LHVP for more than an hour but nucleated particles did not grow above 20 nm (Class II events based on Dal Maso et al., 2005). During the same time, an air ion burst between 2 and 5 nm particle diameter was picked up by the AIS at the same site, but at GOLF the nucleation mode was not observed. The size distribution at SIRTA was not monitored. It is uncertain if nucleation occurred and ions did not grow to detectable size, thus this day was listed as non-event. On July 23 NPF was identified at SIRTA, but at LHVP only the size distribution below 40 nm was monitored by AIS, due to technical issues. Air masses crossed SIRTA before reaching GOLF and a fresh Aitken mode appeared at GOLF three hours later. Wind direction was constant during that period and the lag was consistent with the time needed for an air mass to travel between the two sites at the observed wind speeds (3 m s^{-1}). Similarly to July 23, on July 28 an NPF event was identified at SIRTA and LHVP, while at GOLF a new Aitken mode appeared after approximately three hours. From all this, it can be concluded that the event frequency difference between GOLF and the other two sites can be explained to a large extent by local interferences and uncertainty in identifying nucleation events.

Inhomogeneities with respect to the extent of NPF between locations a few tens of kilometers away, similar to this work, have been reported before (Wehner et al., 2007) and were attributed to cloud cover in combination with a boundary layer evolution scheme that allowed such behavior. However, in the cases investigated in this work, cloud cover did not appear to dictate non-event days at GOLF. Additionally, the beginning of events at all sites always coincided, unlike the cases reported by Wehner et al. (2007). Despite these differences, that work also noted the importance of CS in urban areas.

7. Airborne Measurements

Airborne measurements of N_{10} during summer and winter showed increased number concentrations downwind of Paris accompanied by increases in light absorption measured by the PSAP (Fig. 12). These results were attributed to PM emissions of Paris and are referred henceforth to as the “Paris plume”. This plume identification method assumes that the only black carbon source in the area under investigation is the greater Paris region. However, local sources of black carbon, such as wildfires during summer or domestic heating during winter could interfere. To investigate the validity of our assumption, fire maps derived from satellite information, utilizing a detection algorithm that includes small fires (Randerson et al., 2012), were examined for the two periods (summer and winter) under investigation. During both periods no biomass burning activity was identified ruling out interferences due to this source. During winter, areas where simultaneous increases in absorption and number concentration were identified and attributed to local sources and not the Paris plume. The particle number concentrations in these areas were relatively low though. The potential interference of these sources has a modest to small effect on our estimates regarding the evolution of the Paris aerosol number plume. A similar method of plume identification that involves aerosol absorption was also implemented by Freney et al. (2014) for the same campaign. Increased concentrations of toluene and benzene, both of which are anthropogenic, were also encountered in these plumes.

Due to air traffic restrictions, the ATR-42 was not allowed to get closer than 30 km to the Paris center, but the Paris plume could be identified as far as 200 km away from the city. As stated earlier, airborne measurements were conducted on days when pollution levels were above average and the flight paths were determined a priori based on forecasted values of the numerical model CHIMERE, thus the sample is positively biased. Mobile laboratories on the ground sampled closer to Paris during the whole campaign, but separating the plume from the background was cumbersome (von der Weiden-Reinmüller et al., 2014a).

During summer the averaged aircraft measured N_{10} within the Paris plume was $10.1\pm5.6\times10^{3}$ cm^{-3}, which was 14% higher than the concentrations observed outside of the Paris plume ($8.8\pm6.5\times10^{3}$ cm^{-3}), defining the background concentrations. The high background number concentrations in this N to E quadrant where all of the summer flights but one took place (grey, blue and green lines in Fig. 2) are consistent with the ground (stationary and mobile) observations.

During all summer flights, with the exception of July 25, "hot spots" outside of the Paris plume where particle number concentrations similar to or higher than those of the Paris plume were identified without increase in black carbon or anthropogenic volatile organic compounds (VOCs; benzene, toluene). The "hot spots" where the particle number increase occurred were separated into three groups based on their location with respect to the Paris plume as "upwind", "alongside" and "local".

The "upwind" events were identified upwind of Paris four times, always near IDF (Fig. 12b) and simultaneously with regional nucleation events observed at least at two of the ground sites. The number concentration increases were thus attributed to NPF. Assessment of the spatial extension of these events was complicated by the presence of the plume and limited by the designated flight paths (Fig. 2). In general, the N_{10} measured upwind was 40% higher than that measured in the plume during these "upwind" NPF events.

The "alongside" events occurred at an average distance of 40 km from the plume edge and were attributed to NPF (Fig. 12d). The average number concentration increased by 47% in comparison to the concentration within the Paris plume. The area in between the Paris plume and the hot spot area always exhibited at least 20% lower concentrations than the latter two (Fig. 12d shows the number concentration with respect to cardinal coordinates and Suppl. Fig. 4 as a time-series). The alongside events occurred during four flights (July 1, 15, 21, and 28), two of which were non-event days for all ground sites and two when NPF was identified at SIRTA and LHVP, but not at GOLF. The high N_{10} areas covered approximately 3,000 km^2 along the plume.

In order to investigate why the alongside events occurred only on one side of the Paris plume during these flights, each flight path was separated into three areas: (1) the area with high N_{10} outside of the plume, (2) the plume area and (3) the area on the other side of the plume, where no increase in particle number was observed. The observed differences between both sides of the Paris plume with respect to the CS, solar intensity and isoprene concentration, which has been reported as a potential inhibitor of NPF in forested areas (Kiendler-Scharr et al., 2009; Kanawade et al., 2011), were 12%, 5% and 6%, respectively (Suppl. Fig. 5). These relatively small differences probably cannot explain the observed phenomenon. Other pollutants such as benzene, toluene, monoterpenes, methacrolein, methyl vinyl ketone, O_3, CO, but also meteorological parameters such as temperature and RH were investigated in order to identify potential reasons for the different particle number concentrations between both sides of the plume. Differences in all the investigated parameters were less than 10%. These events clearly require more investigation with instrumentation that can sample particles smaller than 10 nm in combination with trace gas measurements relevant to NPF (e.g. SO_2). Unfortunately, there were no ground measurements in the areas in which the alongside events were identified.

The "local" events were the most frequent (6 out of the 11 study cases) and occurred either at the north coast of France downwind of the city of Fecamp (4 events) and were associated with high or medium tide height (indicating influence of ship emissions?), or near the city of Aulnoye-Aymeries (4 events). On two occasions these events were identified on both locations during the same flight. Because the local events were always associated with specific areas, the particle number concentration increase was attributed to local sources.

During the three winter flights, the Paris plume $N_{2.5}$ was 45% higher than the background and no "hot spots" were identified, consistent with ground measurements where no NPF was identified.

8. Summary and conclusions

Ambient aerosol number concentrations were monitored at the center of Paris (LHVP) along with two satellite suburban stations (SIRTA, SW and GOLF, NE). Mobile measurements were performed by two mobile laboratories and the SAFIRE aircrafts during July 2009 (summer, ATR-42) and January - February 2010 (winter, Piper-Aztec).

During summer, $N_{10\text{-}500}$ (number concentration for particles between 10 and 500 nm diameter) at the city center was lower by 14% than at the downwind (GOLF) and 54% higher than at the upwind (SIRTA) suburban site, respectively. The contribution of particles with diameters between 10 and 30 nm to $N_{10\text{-}500}$ increased from the mostly upwind suburban site (30% at SIRTA) over the city center (40% at LHVP) to the mostly downwind suburban site (50% at GOLF). The contribution of particles with diameters between 30 and 100 nm ranged between 40-50% and followed the opposite trend (highest upwind, lowest downwind).

During summer at SIRTA, $N_{10\text{-}500}$ increased to $9.9\pm2.4\times10^3$ cm^{-3} when the site was downwind of Paris and decreased to $4.2 \pm2.5\times10^3$ cm^{-3} when the site was upwind. At GOLF, located at approximately the same distance from the city center as SIRTA but in the opposite direction (NE), the effect of Paris emissions was not clear, suggesting a high background $N_{10\text{-}500}$ at the measurement location for all wind directions.

NPF events were observed at all sites during summer. At SIRTA and LHVP, events were identified every second day and at GOLF once every four days on average. The lower frequency of NPF events at GOLF was mainly due to interferences from nearby traffic and instrumental limitations which did not allow clear event identification. NPF occurred during periods when the CS was lower by 45%, 25% and 50% at SIRTA, LHVP and GOLF, respectively, in comparison to each site's average value, indicating that the CS may have been a controlling factor for the frequency of events. Solar intensity was higher by 30% and 20% on event days compared to non-event days at SIRTA and LHVP, respectively. At GOLF, solar intensity was higher by 8% during non-event days compared to event days. On average, NPF events caused $N_{10\text{-}500}$ to double at all stationary measurement sites.

Average particle growth rates were 5.5, 4.6 and 6.1 nm h^{-1} at SIRTA, LHVP and GOLF, respectively. The differences between these average growth rates were not statistically significant.

The particle number concentration within the Paris emission plume was found to decrease exponentially on the ground with distance from the Paris center during both campaigns. At distances from the city center greater than 70 km, $N_{2.5}$ was approximately 1.4×10^{4} cm^{-3} regardless of season or whether the measurements were affected by the Paris plume. However during summer background conditions (not affected by Paris), $N_{2.5}$ close to GOLF (second circle in Fig. 1) was approximately a factor of two higher, in agreement with $N_{10\text{-}500}$ measurements at GOLF that indicated a higher background in the region NE of Paris.

The Paris plume was identified by aircraft measurements at an altitude of 600 m, using black carbon as a tracer, as far as 200 km away from the city center. Averaged N_{10} outside and within the Paris plume were $8.8\pm6.5\times10^{3}$ and $10.1\pm5.6\times10^{3}$ cm^{-3}, respectively which corresponds to a 33% increase. During summer, "hot spots" of high particle number concentrations were identified outside of the Paris plume at 600 m altitude. On four occasions the particle number concentration increase was located upwind of the ground stations simultaneously with regional NPF observed on the ground at least at two of the sites. These increases therefore were attributed to NPF. Increased particle number concentrations were also identified along one side of the plume on four occasions. A number of parameters were investigated including CS, solar irradiance, anthropogenic and biogenic VOC concentrations among others, as possible explanations for this asymmetry. All differences observed between both sides of the Paris plume were approximately 10% or lower, so none of these could explain the observations.

During winter the absolute $N_{10\text{-}500}$ was higher by a factor of two at both suburban sites and by 36% at the city center compared to summer. At LHVP particles from 10 to 30 nm accounted for 44% of the $N_{10\text{-}500}$ on average and those from 30 to 100 nm for 40%. At GOLF, similar to summer, the $N_{10\text{-}500}$ was dominated by particles with diameters between 10 and 30 nm which accounted for 56%, followed by particles from 30 to 100 nm (33%), following the same trends as during summer. At SIRTA the contribution of particles from 10 to 30 nm and from 30 to 100 nm to the $N_{10\text{-}500}$ was 42% and 39%, respectively. Regardless of site or season a mode, centered at a diameter below 20 nm, was always present and was dominating during winter at all sites. During winter the higher CS and lower solar intensity compared to summer prevented particles from growing to sizes larger than 10 nm.

A complete year of air ion measurements (including the two intensive campaigns discussed in the present paper) has been recently presented by Dos Santos et al. (2015). These measurements took place in the MEGAPOLI site in the center of Paris (LHVP station) from July 2009 to September 2010. During this year, the highest NPF frequency in Paris was observed during July 2009 (the summer campaign examined in this work) and the lowest during the winter (which includes the winter campaign in this work). Therefore our analysis above focused on two extreme NPF periods in Paris. During summer under clean conditions and peak NPF frequency and during winter under polluted conditions and minimal NPF frequency.

Acknowledgements. Parts of the research leading to these results have received funding from the European Union's Seventh Framework Programme FP7 within the project MEGAPOLI, grant agreement no. 212520 and the FP7 IDEAS project ATMOPACS. The research conducted by MPIC was supported by internal funds. Support from the French ANR project MEGAPOLI – PARIS (ANR-09-BLAN-0356) and from the CNRS-INSU/FEFE via l'ADEME (n° 0962c0018) is acknowledged. We are grateful for the logistical support in the field by IPSL/SIRTA, by Laboratoire d'Hygiène de la Ville de Paris (LHVP) and by the staff of the Golf Départemental de la Poudrerie. The SAFIRE team is acknowledged and thanked for performing ATR-42 flights and measurements.

9. References

Aalto, P. P., Hämeri, K., Becker, E., Weber, R., Salm, J., Mäkelä, J.M., Hoell, C., O'Dowd, C.D., Karlsson, H., Hansson, H.-C., Väkevä, M., Koponen, I.K., Buzorius, G., and Kulmala, M.: Physical characterization of aerosol particles during nucleation events, Tellus, 53B, 344-358, 2001.

Alam, A., Shi, J. P. and Harrison, R. M.: Observations of new particle formation in urban air, J. Geophys. Res., 108, 4093, doi:10.1029/2001JD001417, 2003.

Baklanov, A., Lawrence, M., Pandis, S., Mahura, A., Finardi, S., Moussiopoulos, N., Beekmann, M., Laj, P., Gomes, L., Jaffrezo, J.-L., Borbon, A., Coll, I., Gros, V., Sciare, J., Kukkonen, J., Galmarini, S., Giorgi, F., Grimmond, S., Esau, I., Stohl, A., Denby, B., Wagner, T., Butler, T., Baltensperger, U., Builtjes, P., van den Hout, D., van der Gon, H. D., Collins, B., Schluenzen, H., Kulmala, M., Zilitinkevich, S., Sokhi, R., Friedrich, R., Theloke, J., Kummer, U., Jalkinen, L., Halenka, T., Wiedensholer, A., Pyle, J., and Rossow, W. B.: MEGAPOLI: concept of multi-scale modelling of megacity impact on air quality and climate, Adv. Sci. Res., 4, 115-120, doi:10.5194/asr-4-115-2010, 2010.

Baltensperger, U., Streit, N., Weingartner, E., Nyeki, S., Prévôt, A. S. H., Van Dingenen, R., Virkkula, A., Putaud, J. P., Even, A., Brink, H., Blatter, A., Neftel, A., and Gaggeler, H. W.: Urban and rural aerosol characterization of summer smog events during the PIPAPO field campaign in Milan, Italy, J. Geophys. Res.-Atmos., 107, 8193, 10.1029/2001JD001292, 2002.

Beekmann, M., Prévôt, A. S. H., Drewnick, F., Sciare, J., Pandis, S. N., Denier van der Gon, H. A. C., Crippa, M., Freutel, F., Poulain, L., Ghersi, V., Rodriguez, E., Beirle, S., Zotter, P., von der Weiden-Reinmüller, S.-L., Bressi, M., Fountoukis, C., Petetin, H., Szidat, S., Schneider, J., Rosso, A., El Haddad, I., Megaritis, A., Zhang, Q. J., Michoud, V., Slowik, J. G., Moukhtar, S., Kolmonen, P., Stohl, A., Eckhardt, S., Borbon, A., Gros, V., Marchand, N., Jaffrezo, J. L., Schwarzenboeck, A., Colomb, A., Wiedensohler, A., Borrmann, S., Lawrence, M., Baklanov, A., and Baltensperger, U.: In-situ, satellite measurement and model evidence for a dominant regional contribution to fine particulate matter levels in the Paris Megacity, Atmos. Chem. Phys. Discuss., 15, 8647-8686, doi:10.5194/acpd-15-8647-2015, 2015.

Bermúdez, V., Luján, J., Ruiz, S., Campos, D. and Linares, W.: New European driving cycle assessment by means of particle size distributions in a light-duty diesel engine fuelled with different fuel formulations, Fuel, 140, 649659, doi:10.1016/j.fuel.2014.10.016, 2015.

Barbone, F., Bovenzi, M., Cavallieri, F. and Stanta. G.: Air pollution and lung cancer in Trieste, Italy, Am. J. Epidemiol., 141, 1161-1169, 1995.

Beeson, W. L., Abbey, D.E. and Knutsen. S.F.: Long term concentrations of ambient air pollutants and incident lung cancer in California adults: results from the ASMOGH study, Environ. Health. Perspect. 106, 813-822, 1998.

Birmili, W., Stratmann, F., and Wiedensohler, A.: Design of a DMA-based size spectrometer for a large particle size range and stable operation, J. Aerosol Sci., 30, 549–553, doi:10.1016/S0021-8502(98)00047-0, 1999.

Birmili, W. and Wiedensohler, A.: New particle formation in the continental boundary layer: meteorological and gas phase parameter influence. Geophys. Res. Lett., 27, 3325–3328, 2000.

Bukowiecki, N., Dommen, J., Prévôt, A. S. H., Richter, R., Weingartner, E., and Baltensperger, U.: A mobile pollutant measurement laboratory - measuring gas phase and aerosol ambient concentrations with high spatial and temporal resolution, Atmos. Environ., 36, 5569–5579, 2002.

Bukowiecki, N., Dommen, J., Prévôt, A. S. H., Weingartner, E., and Baltensperger, U.: Fine and ultrafine particles in the Zürich (Switzerland) area measured with a mobile laboratory: an assessment of the seasonal and regional variation throughout a year, Atmos. Chem. Phys., 3, 1477-1494, doi:10.5194/acp-3-1477-2003, 2003.

Bukowiecki, N., Hill, M., Gehrig, R., Zwicky, C., Lienemann, P., Hegedüs, F., Falkenberg, G., Weingartner, E. and Baltensperger, U.: Trace metals in ambient air: Hourly size-segregated mass concentrations determined by Synchrotron-XRF, Environ. Sci. Technol., 39, 5754-5762, doi:10.1021/es048089m, 2005.

Carslaw, K. S., Clegg, S. L., and Brimblecombe, P.: A thermodynamic model of the system $HCl-HNO_3-H_2SO_4-H_2O$, including solubilities of HBr, from <200 K to 328 K, J. Phys. Chem., 99, 11557–11574, 1995.

Chan, T. and Mozurkewich, M.: Application of absolute principal component analysis to size distribution data: identification of particle origins, Atmos. Chem. Phys., 7, 887–897, doi:10.5194/acp-7-887-2007, 2007.

Chung, C. E., Ramanathan, V., Kim, D., and Podgorny, I.: Global anthropogenic aerosol direct forcing derived from satellite and ground-based observations, J. Geophys. Res**.,** 110, D24207, doi:10.1029/2005JD006356, 2005.

Clegg, S., Brimblecombe, L., P. and Wexler, A. S.: A thermodynamic model of the system $H^+-NH_4^+-SO_4^{2-}-NO_3^--H_2O$ at tropospheric temperatures, J. Phys. Chem., A102, 2137–2154, doi:10.1021/jp973043j, 1998.

Couvidat, F., Kim, Y., Sartelet, K., Seigneur, C., Marchand, N., and Sciare, J. : Modeling secondary organic aerosol in an urban area: Application to Paris, France, Atmos. Chem. Phys.,13, 983-996, 2013.

Crippa, M., P.F. DeCarlo, J.G. Slowik, C. Mohr, M.F. Heringa, R. Chirico, L. Poulain, F. Freutel, J. Sciare, J. Cozic, C.F. Di Marco, M. Elsasser, J.B. Nicolas, N. Marchand, E. Abidi, A. Wiedensohler, F. Drewnick, J. Schneider, S. Borrmann, E. Nemitz, R. Zimmermann, J.L. Jaffrezo, A.S.H. Prévôt, U. Baltensperger, Wintertime aerosol chemical composition and source apportionment of the organic fraction in the metropolitan area of Paris, Atmos. Chem. Phys., 13, 961-981, 2013a.

Crippa, M., Canonaco, F., Slowik, J. G., El Haddad, I., DeCarlo, P. F., Mohr, C., Heringa, M., Chirico, R., Marchand, N., Temime, B., Poulain, L., Baltensperger, U., and Prévôt, A. S. H.: Primary and secondary organic aerosols origin by combined gas-particle phase source apportionment, Atmos. Chem. Phys., 13, 8411-8426, 2013b.

Crumeyrolle S., H.E. Manninen, A. Schwarzenboeck, L. Gomes, G. Roberts, M. Kulmala, K. Sellegri, P. Laj. New particle formation events measured by the ATR-42 during the EUCAARI campaign. Atmos. Chem. Phys., 10, 6721-6735, 2010.

Dal Maso, M., Kulmala, M., Lehtinen, K., Mäkelä, J., Aalto, P. and O'Dowd, C.: Condensation and coagulation sinks and formation of nucleation mode particles in coastal and boreal forest boundary layers, J. Geophys. Res.: Atmos., 107, PAR 2-1–PAR 2-10, doi:10.1029/2001JD001053, 2002.

Dal Maso, M., Kulmala, M., Riipinen, I., Wagner, R., Hussein, T., Aalto, P., and Lehtinen, K. E. J.: Formation and growth of fresh atmospheric aerosols: Eight years of aerosol size distribution data from SMEAR II, Hyytiälä, Finland, Boreal Environ. Res., 10, 323–336, 2005.

Dos Santos, V. N., Herrmann, E., Manninen, H. E., Hussein, T., Hakala, J., Nieminen, T., Aalto, P. P., Merkel, M., Wiedensohler, A., Kulmala, M., Petäjä, T., and Hämeri, K.: Variability of air ion concentrations in urban Paris, Atmos. Chem. Phys. Discuss., 15, 10629-10676, doi:10.5194/acpd-15-10629-2015, 2015.

Drewnick, F., Böttger, T., von der Weiden-Reinmüller, S.-L., Zorn, S. R., Klimach, T., Schneider, J., and Borrmann, S.: Design of a mobile aerosol research laboratory and data processing tools for effective stationary and mobile field measurements, Atmos. Meas. Tech., 5, 1443-1457, doi:10.5194/amt-5-1443-2012, 2012.

Dunn, M.J., Jimenez, J.L., Baumgardner, D., Castro, T., McMurry, P.H., Smith, J.N.: Measurements of Mexico City nanoparticle size distributions: observations of new particle formation and growth. Geophys. Res. Lett., 31, L10102, doi:10.1029/2004GL019483, 2004.

Engelhart, G. J., Hildebrandt, L., Kostenidou, E., Mihalopoulos, N., Donahue, N. M., and Pandis, S. N.: Water content of aged aerosol, Atmos. Chem. Phys., 11, 911-920, doi:10.5194/acp-11-911-2011, 2011.

Favez, O., Cachier, H., Sciare, J., Le Moullec, Y.: Characterization and contribution to $PM_{2.5}$ of semi-volatile aerosols in Paris (France), Atmos. Environ., 41, 7969-7976, 2007.

Freney, E. J., Sellegri, K., Canonaco, F., Colomb, A., Borbon, A., Michoud, V., Doussin, J.-F., Crumeyrolle, S., Amarouche, N., Pichon, J.-M., Bourianne, T., Gomes, L., Prévôt, A. S. H., Beekmann, M., and Schwarzenböeck, A.: Characterizing the impact of urban emissions on regional aerosol particles: airborne measurements during the MEGAPOLI experiment, Atmos. Chem. Phys., 14, 1397-1412, 2014.

Freutel, F., Schneider, J., Drewnick, F., von der Weiden-Reinmüller, S.-L., Crippa, M., Prévôt, A. S. H., Baltensperger, U., Poulain, L., Wiedensohler, A., Sciare, J., Sarda-Estève, R., Burkhart, J. F., Eckhardt, S., Stohl, A., Gros, V., Colomb, A., Michoud, V., Doussin, J. F., Borbon, A., Haeffelin, M., Morille, Y., Beekmann, M., and Borrmann, S.: Aerosol particle measurements at three stationary sites in the megacity of Paris during summer 2009: meteorology and air mass origin dominate aerosol particle composition and size distribution, Atmos. Chem. Phys., 13, 933-959, 2013.

Fuchs, N., and A. Sutugin, Highly dispersed aerosol, in Topics in Current Aerosol Research, edited by G. Hidy, and J. Brock, Pergamon, New York, 1971.

Gurjar, B. R., Butler, T. M., Lawrence, M. G., and Lelieveld, J.: Evaluation of emissions and air quality in megacities, Atmos. Environ., 42, 1593–1606, 2008.

Hering, S. V., Kreisberg, N. M., Stolzenburg, M. R., and Lewis, G. S.: Comparison of particle size distributions at urban and agricultural sites in California's San Joaquin Valley, Aerosol Sci. Technol., 41, 86-96, 2007.

Hirsikko, A., Laakso, L., Hõrrak, U., Aalto, P., Kerminen, V.-M., and Kulmala, M.: Annual and size dependent variation of growth rates and ion concentrations in boreal forest, Boreal Environ. Res., 10, 357–369, 2005.

Hirsikko, A., Bergman, T., Laakso, L., Dal Maso, M., Riipinen, I., Hõrrak, U., and Kulmala, M.: Identification and classification of the formation of intermediate ions measured in boreal forest, Atmos. Chem. Phys., 7, 201–210, 2007.

Hirsikko, A., Vakkari, V., Tiitta, P., Manninen, H. E., Gagné, S., Laakso, H., Kulmala, M., Mirme, A., Mirme, S., Mabaso, D., Beukes, J. P., and Laakso, L.: Characterisation of sub-micron particle number concentrations and formation events in the western Bushveld Igneous Complex, South Africa, Atmos. Chem. Phys., 12, 3951-3967, 2012.

Hussein, T., Puustinen, A., Aalto, P., Mäkelä, J., Hämeri, K. and Kulmala, M.: Urban aerosol number size distributions, Atmos. Chem. Phys., 4, 391–411, doi:10.5194/acp-4-391-2004, 2004.

IPCC 2007 *Fourth Assessment Report (IPCC AR4)* (Geneva: Intergovernmental Panel on Climate Change), 2007.

Jayne, J.T., Leard, D.C., Zhang, X., Davidovits, P., Smith, K. A., Kolb, C. E., and Worsnop, D. R.: Development of an aerosol mass spectrometer for size and composition analysis of submicron particles, Aerosol Sci. Technol., 33, 49–70, 2000.

Jimenez, J. L., Jayne, J. T., Shi, Q., Kolb, C. E., Worsnop, D. R., Yourshaw, I., Seinfeld, J. H., Flagan, R. C., Zhang, X., Smith, K. A., Morris, J., and Davidovits, P.: Ambient aerosol sampling using the Aerodyne Aerosol Mass Spectrometer, J. Geophys. Res., 108, 8425, doi:10.1029/2001JD001213, 2003.

Junninen, H., Hulkkonen, M., Riipinen, I., Nieminen, T., Hirsikko, A., Suni, T., Boy, M., Lee, S.-H., Vana, M., Tammet, H., Kerminen, V.-M., and Kulmala, M.: Observations on nocturnal growth of atmospheric clusters, Tellus, 60B, 365–371, 2008.

Kalivitis N., I. Stavroulas, A. Bougiatioti, G. Kouvarakis, S. Gagne, H. E. Manninen, M. Kulmala, and Mihalopoulos, N.: Night-time enhanced atmospheric ion concentrations in the marine boundary layer, Atmos. Chem. Phys., 12, 3627–3638, 2012.

Kanawade, V. P., B. T. Jobson, A. B. Guenther, M. E. Erupe, S. N. Pressley, S. N. Tripathi, and Lee, S.-H.: Isoprene suppression of new particle formation in a mixed deciduous forest, Atmos. Chem. Phys., 11, 6013–6027, 2011.

Kiendler-Scharr, A., Wildt, J., Dal Maso, M., Hohaus, T., Kleist, E., Mente, T. F., Tillmann, R., Uerlings, R., Schurr, U., and Wah-ner, A.: New particle formation in forests inhibited by isoprene emissions, Nature, 461, 381–384, 2009.

Komppula, M., Sihto, S.-L., Korhonen, H., Lihavainen, H., Kerminen, V.-M., Kulmala, M., and Viisanen, Y.: New particle formation in air mass transported between two measurement sites in Northern Finland, Atmos. Chem. Phys., 6, 2811-2824, 2006.

Kulmala, M., Dal Maso, M., Mäkelä, J., Pirjola, L., Väkevä, M., Aalto, P., Miikkulainen, P., Hämeri, K. and O'Dowd, C.: On the formation, growth and composition of nucleation mode particles, Tellus B, 53(4), 479–490, doi:10.1034/j.1600-0889.2001.530411.x, 2001.

Kulmala, M., Vehkamaki, H., Petaja, T., Dal Maso, M., Lauri, A., Kerminen, V. M., Birmili, W., and McMurry, P. H.: Formation and growth rates of ultrafine atmospheric particles: a review of observations, J. Aerosol Sci., 35, 143–176, 2004.

Laakso, L., Hussein, T., Aarnio, P., Komppula, M., Hiltunen, V., Viisanen, Y., and Kulmala, M.: Diurnal and annual characteristics of particle mass and number concentrations in urban, rural and arctic environments in Finland, Atmos. Environ. 37, 2629–2641, 2003.

Laden, F., Schwartz, J., Speizer, F. E., and Dockery, D.: Reduction in fine particulate air pollution and mortality: Extended followup of the Harvard Six Cities Study, Am. J. Respir. Crit. Care Med., 173, 667–672, doi:10.1164/rccm.200503-443OC, 2006.

Lawrence, M. G., Butler, T. M., Steinkamp, J., Gurjar, B. R., and Lelieveld, J.: Regional pollution potentials of megacities and other major population centers, Atmos. Chem. Phys., 7, 3969–3987, 2007.

Lohmann U. and Feichter J.: Global indirect aerosol effects: a review, Atmos. Chem. Phys., 5, 715–737, 2005.

Manninen, H. E., Nieminen, T., Asmi, A., et al.: EUCAARI ion spectrometer measurements at 12 European sites – analysis of new-particle formation events, Atmos. Chem. Phys. 10, 7907–7927, 2010.

Massucci, M., Clegg, S. L., and Brimblecombe, P.: Equilibrium partial pressures, thermodynamic properties of aqueous and solid phases, and Cl_2 production from aqueous HCl and HNO_3 and their mixtures, J. Phys. Chem. A, 103, 4209–4226, 1999.

Mauldin, R., Cantrell, C., Zondlo, M., Kosciuch, E., Eisele, F., Chen, G., Davis, D., Weber, R., Crawford, J., Blake, D., Bandy, A. and Thornton, D.: Highlights of OH, H_2SO_4, and methane sulfonic acid measurements made aboard the NASA P-3B during Transport and Chemical Evolution over the Pacific, J. Geophys. Res., 108, 8796–8808, doi:10.1029/2003JD003410, 2003.

McNaughton, C. S., Clarke, A. D., Howell, S. G., Pinkerton, M., Anderson, B., and Thornhill, L.: Results from the DC-8 Inlet Characterization Experiment (DICE): Airborne versus surface sampling of mineral dust and sea salt aerosols. Aerosol Sci. Technol., 41, 136–159, doi:10.1080/02786820601118406, 2007.

Menut L. and Bessagnet, B.: Atmospheric composition forecasting in Europe, Annales Geophysicae, 28, 61-74, 2010.

Menut L, Bessagnet, B., Khvorostyanov, D., Beekmann, M., Blond, N., Colette, A., Coll, I., Curci, G., Foret, G., Hodzic, A., Mailler, S., Meleux, F., Monge, J.L., Pison, I., Siour, G., Turquety, S., Valari, M., Vautard, R. and Vivanco, M.G.: CHIMERE 2013: a model for regional atmospheric composition modelling, Geoscientific Model Development, 6, 981-1028, 2013.

Michoud, V., Kukui, A., M. Camredon, A. Colomb, A. Borbon, K. Miet, B. Aumont, M. Beekmann, R. Durand-Jolibois, S. Perrier, P. Zapf, G. Siour, W. Ait-Helal, N. Locoge, S. Sauvage, C. Afif, V. Gros, M. Furger, G. Ancellet, and J. F. Doussin: Radical budget analysis in a suburban European site during the MEGAPOLI summer field campaign, Atmos. Chem. Phys., 12, 11951-11974, 2012.

Molina, M. J. and Molina, L. T.: Critical Review: Megacities and atmospheric pollution, J. Air Waste Manage. Assoc., 54, 644–680, 2004.

Molina, L. T., Molina, M. J., Slott, R., Kolb, C. E., Gbor, P. K., Meng, F., Singh, R., Galvez, O., Sloan, J. J., Anderson, W., Tang, X. Y., Shao, M., Zhu, T., Zhang, Y. H., Hu, M., Gur-jar, B. R., Artaxo, P., Oyola, P., Gramsch, E., Hidalgo, P., and Gertler A.: Critical Review Supplement: Air quality in selected Megacities, J. Air Waste Manage. Assoc, 12, 1–73, doi:10.1080/10473289.2004.1047101, 2004.

McMurry , P . H., Woo, K. S., Weber, R., Chen, D.-R., and Pui, D. Y. H.: Size Distributions of 3 to 10 nm Atmospheric Particles: Implications for nucleation mechanisms, T. Roy. Soc. Lond. A, 358, 2625–2642, 2000.

McMurry, P. H., Fink, M., Sakuri, H., Stolzenburg, M., Mauldin III, R. L., Smith, J., Eisele, F. L., Moore, K., Sjostedt, S., Tanner, D., Huey, L.G., Nowak, J. B., Edgerton, E., and Voisin, D.: A criterion for new particle formation in the sulfur-rich Atlanta atmosphere, J. Geophys. Res., 110, D22S02, doi:10.1029/2005JD005901, 2005.

Mirme, A., Tamm, E., Mordas, G., Vana, M., Uin, J., Mirme, S., Bernotas, T., Laakso, L., Hirsikko, A., and Kulmala, M.: A wide-range multi-channel Air Ion Spectrometer, Boreal Environ. Res., 12, 247–264, 2007.

Nafstad, P., Haheim, L.L., Oftedal, B., Gram, F., Holme, I., Hjermann, I. and Leren, P.: Lung cancer and air pollution: a 27 years follow-up of 16 209 Norwegian men, Thorax, 58, 1071-1076, 2003.

Nyberg, F., Gustavsson, P., Järup, L., Bellander, T., Berglind, N., Jakobsson, R. and Pershagen, G.: Urban air pollution and lung cancer in Stockholm, Epidemiology, 11, 487-495, 2000.

Organization for Economic Co-operation and Development: Definition of Functional Urban Areas (FUA) for the OECD metropolitan database, available at: http://www.oecd.org/gov/regional-policy/Definition-of-Functional-Urban-Areas-for-the-OECD-metropolitan-database.pdf (last access: 13 February 2015), 2013.

Ortega, I. K., Suni, T., Boy, M., Grönholm, T., Manninen, H. E., Nieminen, T., Ehn, M., Junninen, H., Hakola, H., Hellén, H., Valmari, T., Arvela, H., Zegelin, S., Hughes, D., Kitchen, M., Cleugh, H., Worsnop, D. R., Kulmala, M., and Kerminen, V.-M.: New insights into nocturnal nucleation, Atmos. Chem. Phys., 12, 4297-4312, 2012.

Pierce, J. R., and Adams, P. J.: Can cosmic rays affect cloud condensation nuclei by altering new particle formation rates?, Geophys. Res. Lett., 36, L09820, doi:10.1029/2009GL037946, 2009.

Pikridas, M., Riipinen, I., Hildebrandt, L., Kostenidou, E., Manninen, H. E., Mihalopoulos, N., Kalivitis, N., Burkhart, J. F., Stohl, A., Kulmala, M., and Pandis, S. N.: New particle for-mation at a remote site in the eastern Mediterranean, J. Geophys. Res., 117, D12205, doi:10.1029/2012JD017570, 2012.

Platt, S., Haddad, I., Zardini, A., Clairotte, M., Astorga, C., Wolf, R., Slowik, J., Temime-Roussel, B., Marchand, N., Ježek, I., Drinovec, L., Močnik, G., Möhler, O., Richter, R., Barmet, P., Bianchi, F., Baltensperger, U. and Prévôt, A.: Secondary organic aerosol formation from gasoline vehicle emissions in a new mobile environmental reaction chamber, Atmos. Chem. Phys., 13, 9141–9158, doi:10.5194/acp-13-9141-2013, 2013.

Pope, C.A., Burnett, R.T., Thun, M.J., Calle, E.E., Krewski ,D., Ito, K. and Thurston, G.D.: Lung cancer, cardiopulmonary mortality and long term exposure to fine particulate air pollution, J. Am. Med. Assoc., 287, 1132-1141, 2002.

Pope, C. A., Ezzati, M., and Dockery, D. W.: Fine-particulate air pollution and life expectancy in the United States, New Engl. J. Med. 360, 376–386, 2009..

Randerson, J., Chen, Y., Werf, G., Rogers, B. and Morton, D.: Global burned area and biomass burning emissions from small fires, J. Geophys. Res., 117(G4), doi:10.1029/2012JG002128, 2012.

Riccobono, F., Schobesberger, S., Scott, C., Dommen, J., Ortega, I., Rondo, L., Almeida, J., Amorim, A., Bianchi, F., Breitenlechner, M., David, A., Downard, A., Dunne, E., Duplissy, J., Ehrhart, S., Flagan, R., Franchin, A., Hansel, A., Junninen, H., Kajos, M., Keskinen, H., Kupc, A., Kurten, A., Kvashin, A., Laaksonen, A., Lehtipalo, K., Makhmutov, V., Mathot, S., Nieminen, T., Onnela, A., Petaja, T., Praplan, A., Santos, F., Schallhart, S., Seinfeld, J., Sipila, M., Spracklen, D., Stozhkov, Y., Stratmann, F., Tome, A., Tsagkogeorgas, G., Vaattovaara, P., Viisanen, Y., Vrtala, A., Wagner, P., Weingartner, E., Wex, H., Wimmer, D., Carslaw, K., Curtius, J., Donahue, N., Kirkby, J., Kulmala, M., Worsnop, D. and Baltensperger, U.: Oxidation products of biogenic emissions contribute to nucleation of atmospheric particles, Science, 344, 717-721, 2014.

Rouil, L., Honore, C., Vautard, R., Beekmann, M., Bessagnet, B., Malherbe, L., Meleux, F., Dufour, A., Elichegaray, C., Flaud, J-M., Menut, L., Martin, D., Peuch, A., Peuch, V-H., Poisson, N.: PREV'AIR : an operational forecasting and mapping system for air quality in Europe, BAMS, doi: 10.1175/2008BAMS2390.1, 2009.

Rodríguez, S., Van Dingenen, R., Putaud, J.-P., Roselli, D.: Nucleation and growth of new particles in the rural atmosphere of Northern Italy relationship to air quality monitoring, Atmos. Environ., 39, 6734-6746, 2005.

Ruuskanen, J., Tuch, Th., Ten Brink, H., Peters, A., Khlystov, A., Mirme, A., Kos, G. P. A., Brunekreef, B., Wichmann, H. E., Buzorius, G., Vallius, M., Kreyling, W. G., and Pekkanen, J.: Concentrations of ultrafine, fine and $PM_{2.5}$ particles in three European cities, Atmos. Environ, 35, 3729-3738, 2001.

Sciare, J., d'Argouges, O., Zhang, Q. J., Sarda-Esteve, R., Gaimoz, C., Gros, V., Beekmann, M., and Sanchez, O.: Comparison between simulated and observed chemical composition of fine aerosols in Paris (France) during springtime: contribution of regional versus continental emissions, Atmos. Chem. Phys., 10, 11987–12004, 2010.

Shi, Q.: Aerosol size distributions (3nm to 3mm) measured at the St. Louis Supersite (4/1/01–4/30/02). M.S. Thesis, Department of Mechanical Engineering, University of Minnesota, Minneapolis, MN 55455. 2003.

Shi, Q., Sakurai, H., and McMurry, P. H.: Characteristics of regional nucleation events in urban East St. Louis, Atmos. Environ., 41, 4119–4127, 2007.

Skyllakou, K., Murphy, B. N., Megaritis, A. G., Fountoukis, C., and Pandis, S. N.: Contributions of local and regional sources to fine PM in the megacity of Paris, Atmos. Chem. Phys., 14, 2343-2352, doi:10.5194/acp-14-2343-2014, 2014.

Stanier, C. O., Khlystov, A., and Pandis, S. N.: Nucleation events during the Pittsburgh Air Quality Study: Description and relation to key meteorological, gas-phase, and aerosol parameters, Aerosol Sci. Technol, 38(S1), 253–264, 2004a.

Stanier C. O., Khlystov, A. Y., and Pandis S. N.: Ambient aerosol size distributions and number concentrations measured during the Pittsburgh Air Quality Study, Atmos. Environ., 38, 3275–3284, 2004b.

Stohl, A., Forster, V., Frank, A., Seibert, P., and Wotawa, G.: Technical Note: The Lagrangian particle dispersion model FLEXPART version 6.2, Atmos. Chem. Phys., 5, 2461–2474, 2005.

Tuch, T., Wehner, B., Pitz, M., Cyrys, J., Heinrich, J., Kreyling, W. G., Wichmann, H. E., and Wiedensohler, A.: Long-term measurements of size-segregated ambient aerosol in two German cities located 100 km apart, Atmos. Environ.37, 4687–4700, 2003.

Tuch, T. M., Haudek, A., Müller, T., Nowak, A., Wex, A., and Wiedensohler, A.: Design and performance of an automatic regenerating adsorption aerosol dryer for continuous operation at monitoring sites**,** Atmos. Meas. Tech., 2, 417-422, 2009.

United Nations, Revision of World Urbanization Prospects, New York, 2014.

Vana, M., Kulmala, M., Dal Maso, M., Horrak, U. and Tamm, E.: Comparative study of nucleation mode aerosol particles and intermediate air ions formation events at three sites, J. Geophys. Res. 109, D7201, doi: 10.1029/2003JD004413, 2004.

Vana, M., Ehn, M., Petäjä, T., Vuollekoski, H., Aalto, P., de Leeuw, G., Ceburnis, D., O'Dowd, C. D., and Kulmala, M.: Characteristic features of air ions at Mace Head on the west coast of Ireland, Atmos. Res., 90, 278, doi:10.1016/j.atmosres.2008.04.007, 2008.

von der Weiden-Reinmüller, S.-L., Drewnick, F., Crippa, M., Prévôt, A. S. H., Meleux, F., Baltensperger, U., Beekmann, M., and Borrmann, S.: Application of mobile aerosol and trace gas measurements for the investigation of megacity air pollution emissions: the Paris metropolitan area, Atmos. Meas. Tech., 7, 279-299, 2014a.

von der Weiden-Reinmüller, S.-L., Drewnick, F., Zhang, Q. J., Freutel, F., Beekmann, M., and Borrmann, S.: Megacity emission plume characteristics in summer and winter investigated by mobile aerosol and trace gas measurements: the Paris metropolitan area, Atmos. Chem. Phys., 14, 11931-11250, 2014b.

Wåhlin, P., Palmgren, F., Dingenen, R. and Raes, F.: Pronounced decrease of ambient particle number emissions from diesel traffic in Denmark after reduction of the sulphur content in diesel fuel, Atmos. Environ., 35, 35493552, doi:10.1016/S1352-2310(01)00066-8, 2001.

Wåhlin, Peter.: Measured reduction of kerbside ultrafine particle number concentrations in Copenhagen, Atmos. Environ., 43, 3645–3647, 2009.

Wang, Z., Hopke, P. K., Ahmadi, G., Cheng, Y. S., and Baron, P. A.: Fibrous particle deposition in human nasal passage: The influence of particle length, flow rate, and geometry of nasal airway, J. Aerosol Sci., 39, 1040–1054, 2008.

Wang, F., Costabileb, F., Li, H., Fang, D., Alligrini, I.: Measurements of ultrafine particle size distribution near Rome, Atmos. Res. 98, 69–77, 2010.

Watson, J. G., Chow, J. C., Lowenthal, D. H., Kreisberg, N. M., Hering, S. V., and Stolzenburg, M. R.: Variations of nanoparticle concentrations at the Fresno Supersite, Sci. Tot. Environ., 358, 178–187, 2006.

Wehner, B. and Wiedensohler, A: Long term measurements of submicrometer urban aerosols: statistical analysis for correlations with meteorological conditions and trace gases, Atmos. Chem. Phys. 3, 867-879, 2003.
Wehner, B., Wiedensohler, A., Tuch, T. M., Wu, Z. J., Hu, M., Slanina, J., and Kiang, C. S.: Variability of the aerosol number size distribution in Beijing, China: new particle formation, dust storms, and high continental background, Geophys. Res. Lett., 31, L22108, doi:10.1029/2004GL021596 2004.
Wehner, B., Siebert, H., Stratmann, F., Tuch, T., Wiedensohler, A., Petäjä, T., Dal Maso, M. and Kulmala, M.: Horizontal homogeneity and vertical extent of new particle formation events, Tellus, B, 59, 362–371, doi:10.1111/j.1600-0889.2007.00260.x, 2007.
Weimer, S., C. Mohr, R. Richter, J. Keller, M. Mohr, A. S. H. Prévôt, and U. Baltensperger.: Mobile measurements of aerosol number and volume size distributions in an Alpine valley: Influence of traffic versus wood burning, Atmos. Environ., 43, 624-630, 2009.
Wen, J., Zhao, Y., and Wexler, A. S.: Marine particle nucleation: Observation at Bodega Bay, California, J. Geophys. Res., 111, D08207, doi:10.1029/2005JD006210, 2006.
Woo, K. S., Chen, D. R., Pui, D. Y. H. and McMurry, P. H.: Measurement of Atlanta aerosol size distributions: Observations of ultrafine particle events, Aerosol Sci. Technol., 34, 75-87, 2001.
World Bank: World Development Report 2012: World Development Indicators, Fossil Fuel Energy Consumption, 2012.
Wu, Z.J., Hu, M., Liu, S., Wehner, B., Bauer, S., Maßling, A., Wiedensohler, A., Petaja , T., Dal Maso, M., Kulmala, M.: New particle formation in Beijing, China: statistical analysis of a 1-year data set. J. Geophys. Res., 112, D09209. doi:10.1029/2006JD007406, 2007.
Zhang, Q. J., Beekmann, M., Drewnick, F., Freutel, F., Schneider, J., Crippa, M., Prevot, A. S. H., Baltensperger, U., Poulain, L., Wiedensohler, A., Sciare, J., Gros, V., Borbon, A., Colomb, A., Michoud, V., Doussin, J.-F., Denier van der Gon, H. A. C., Haeffelin, M., Dupont, J.-C., Siour, G., Petetin, H., Bessagnet, B., Pandis, S. N., Hodzic, A., Sanchez, O., Honoré, C., and Perrussel, O.: Formation of organic aerosol in the Paris region during the MEGAPOLI summer campaign: evaluation of the volatility-basis-set approach within the CHIMERE model, Atmos. Chem. Phys., 13, 5767-5790, doi:10.5194/acp-13-5767-2013, 2013.
Zhou, L., Kim, E., Hopke, P., Stanier, C. and Pandis, S.: Advanced Factor Analysis on Pittsburgh Particle Size-Distribution Data, Aerosol Sci. and Technol., 38 (Sup.1), 118-132, doi:10.1080/02786820390229589, 2004.

Table 1. Summary of main MEGAPOLI measurements used in this study.

Variable	Instrument	Group	Time Resolution	Sample Condition
ATR-42				
Absorption (summer)	PSAP[a]	LaMP[j]	1 sec	dry
Trace Gas Concentration	HS PTR-QMS 500[b]	CNRS[k]	1 sec	dry
Aerosol Number Concentration	TSI 3025 CPC[c]	CNRM[l]	1 sec	dry
Aerosol Number Concentration	TSI 3010 CPC[c]	LaMP[j]	1 sec	dry
Absorption (winter)	PSAP[a]	CNRM[l]	1 sec	dry
MoLa				
Aerosol Number Concentration	TSI 3786 UWCPC[d]	MPIC[m]	1 sec	ambient
MOSQUITA				
Aerosol Number Concentration	TSI 3010 CPC[c]	PSI[n]	1sec	ambient
Aerosol Number Concentration	UHSAS[e]	PSI[n]	1 sec	ambient
SIRTA				
Aerosol Number Size Distribution (10–500 nm)	SMPS[f]	CMU[o]	10 min	dry
Aerosol Number Size Distribution (6–800 nm)	DMPS[g]	UoH[p]	9 min	ambient
LHVP				
Aerosol Number Size Distribution (3–630 nm)	DMPS[g]	IfT[q]	10 min	dry
Positive/Negative Ion Size Distribution (0.8–40 nm)	AIS[h]	UoH[p]	3 min	ambient
GOLF				
Aerosol Number Size Distribution (5 nm–1 μm)	EAS[i]	MPIC[m]	1 min	ambient

[a]PSAP: Particle Soot Absorption Photometer; [b]HS PTR-QMS: High Sensitivity Proton Transfer Reaction-Quadrupole Mass Spectrometer; [c]CPC: Condensation Particle Counter; [d]UWCPC: Ultrafind Water Condensation Particle Counter; [e]UHSAS: Ultra High Sensitivity Aerosol Spectrometer; [f]SMPS: Scanning Mobility Particle Sizer; [g]DMPS: Differential Mobility Particle Sizer; [h]AIS: Air Ion Spectrometer; [i]EAS: Electrical Aerosol Spectrometer; [j]LaMP: Laboratoire Meteorologie Physique; [k]CNRS: Centre national de la recherche scientifique; [l]CNRM: Centre National de Recherches Météorologiques; [m]MPIC: Max Planck Institute for Chemistry; [n]PSI: Paul Scherrer Institute; [o]CMU: Carnegie Mellon University; [p]UoH: University of Helsinki; [q]IfT: Leibniz Institute for Tropospheric Research.

Table 2. Aerosol number concentrations during the summer and winter campaigns and characteristics of NPF during summer. σ is the standard deviation.

	Average ± 1σ Number Concentration (10 - 500 nm) 1000/cm^3		Average increase±1σ in Number Concentration due to NPF (%)	Growth Rate ±1σ (nm h^{-1})
Site	*Summer*	*Winter*	*Summer*	*Summer*
GOLF	13.3±6.8	25.3±15.1	127±110	6.1±1.8
LHVP	11.4±5.1	15.6±7.1	100±50	4.6±1.9
SIRTA	5.3±3.1	10.1±5.7	129±59	5.5±4.1

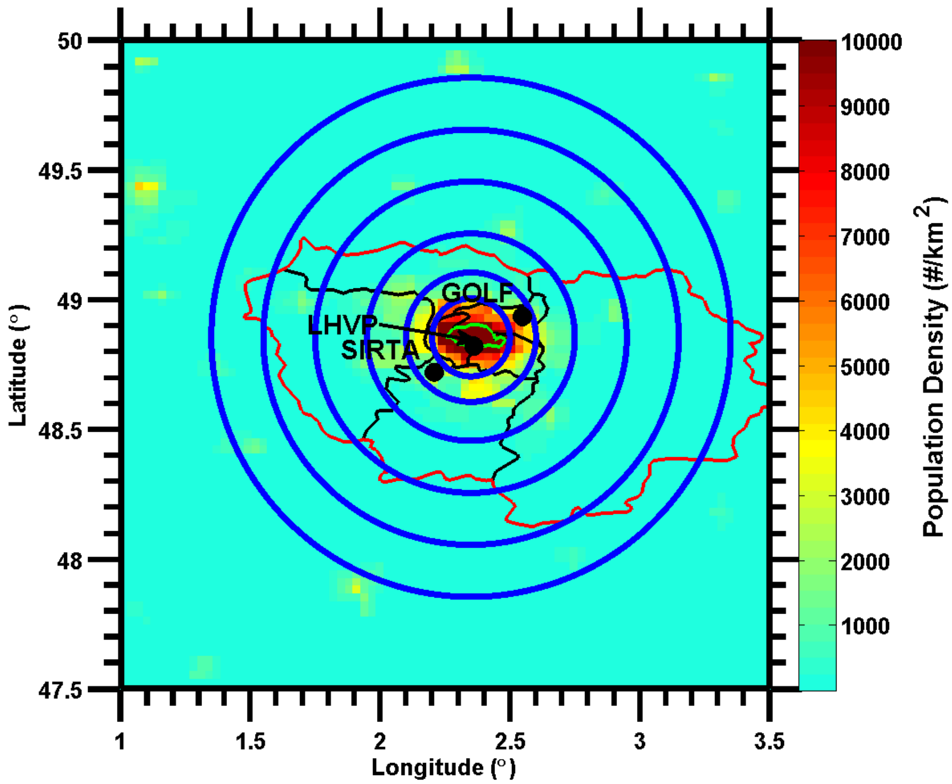

Fig. 1. Population density and administrative map of Paris. Outlined in red is Île de France and in green Paris. The three ground stations (SIRTA, LHVP and GOLF) are depicted with black dots. The map is separated into sectors depicted by blue lines, formed by concentric circles centered at kilometer zero of Paris (48.8534 °N 2.3488 °E). The radius of the circles is 0.15, 0.25, 0.4, 0.6, 0.8 and 1 °, which corresponds to 16.7, 27.8, 44.4, 66.7, 88.9 and 111.1 km.

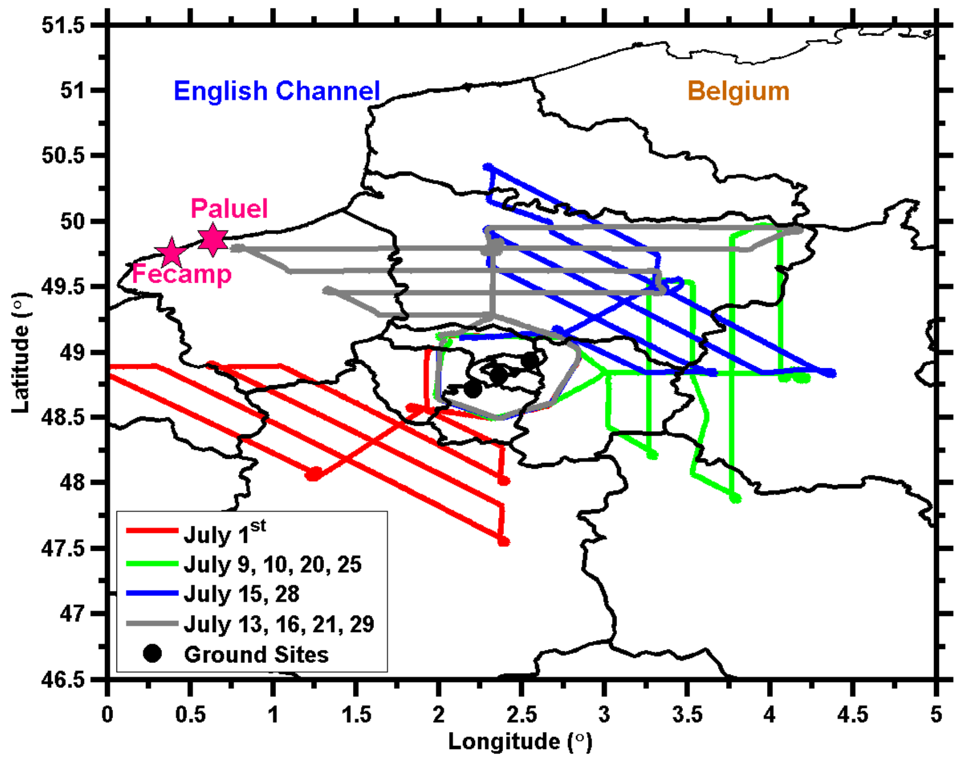

Fig. 2. Flight paths of the ATR-42 aircraft during the summer campaign. Different colors correspond to different flight routes. The cities of Fecamp and Paluel are also depicted in the map.

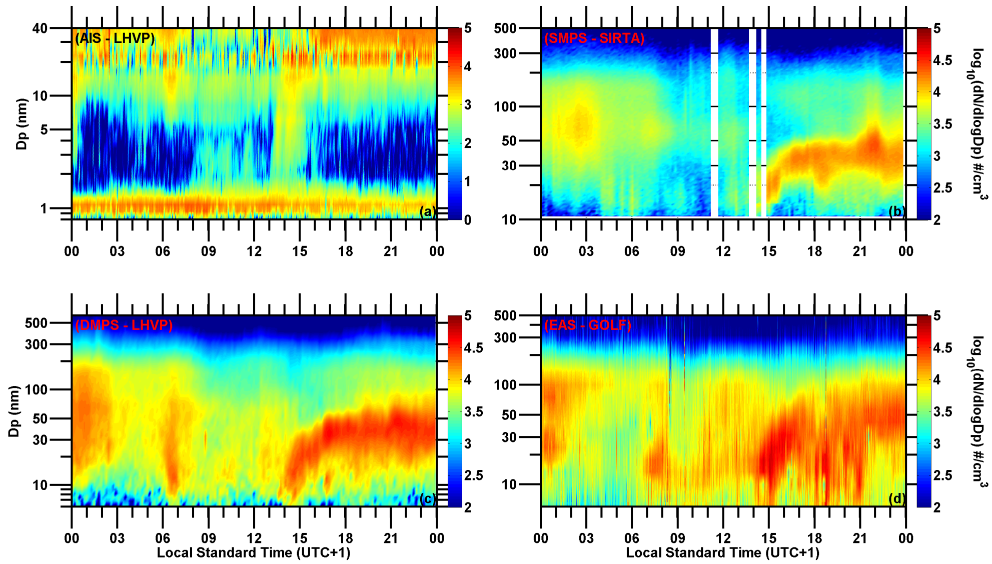

Fig. 3. Size distribution measurements during a nucleation event day (12 July 2009) at all ground sites. (a) AIS measurements at LHVP, (b) SMPS measurements at SIRTA, (c) DMPS measurements at LHVP, (d) EAS measurements at GOLF. Time of day corresponds to local standard time (UTC+1). D_p is the particle diameter.

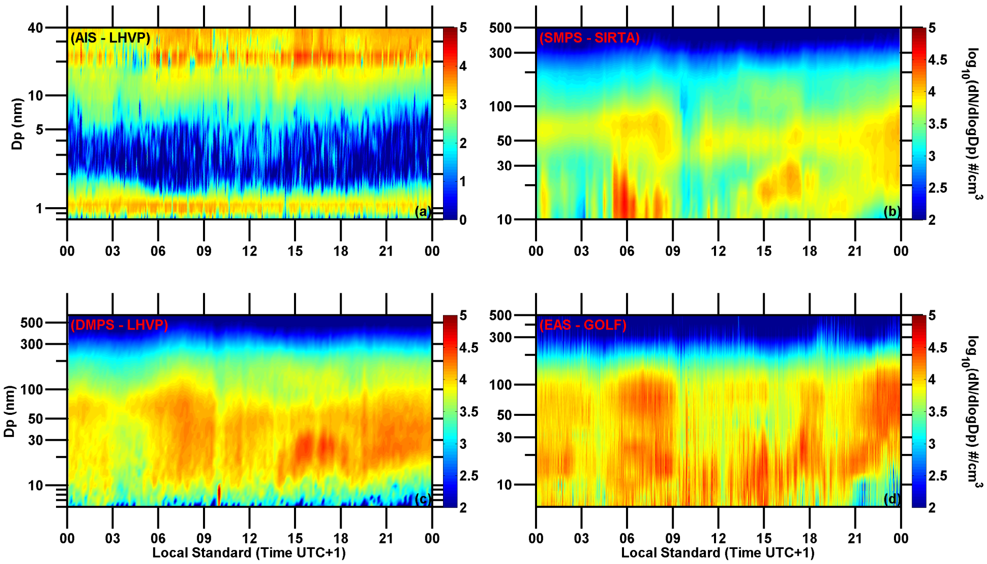

Fig. 4. Size distribution measurements during an undefined event day (10 July 2009): (a) AIS measurements at LHVP, (b) SMPS measurements at SIRTA, (c) DMPS measurements at LHVP, (d) EAS measurements at GOLF. Time of day corresponds to local standard time (UTC+1). D_p is the particle diameter.

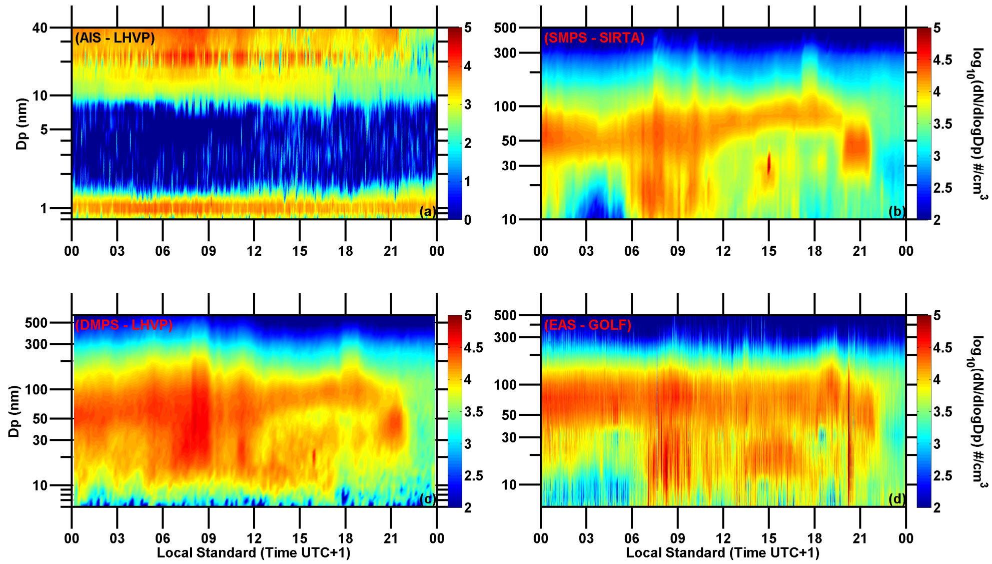

Fig. 5. Size distribution measurements during a non-event day (29 July 2009): (a) AIS measurements at LHVP, (b) SMPS measurements at SIRTA, (c) DMPS measurements at LHVP, (d) EAS measurements at GOLF. Time of day corresponds to local standard time (UTC+1). D_p is the particle diameter.

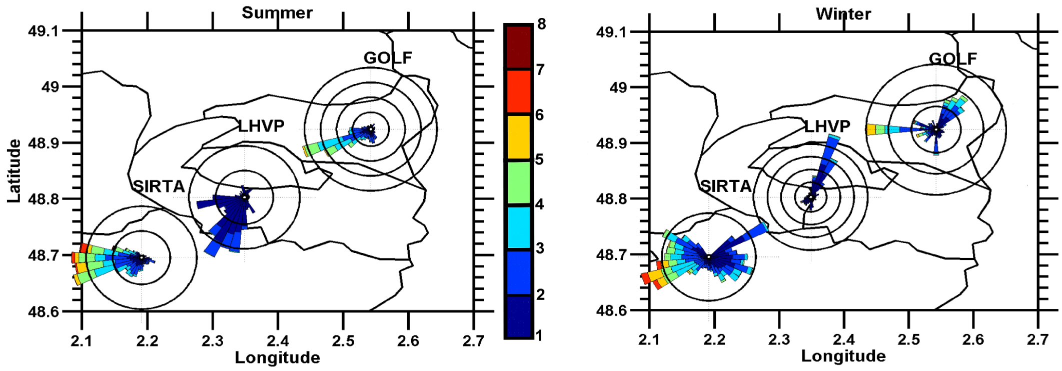

Fig. 6. Wind direction rose plots during the summer and winter campaigns at each of the ground sites. Each rose segment corresponds to an angle bin of $\pi/18$ (i.e. 20°) and concentric circles at each site correspond to 5% relative frequency. Wind speed, in m s^{-1}, corresponding to each size bin is color coded inside each rose. Wind speeds below 1 m s^{-1} have been omitted from the graph.

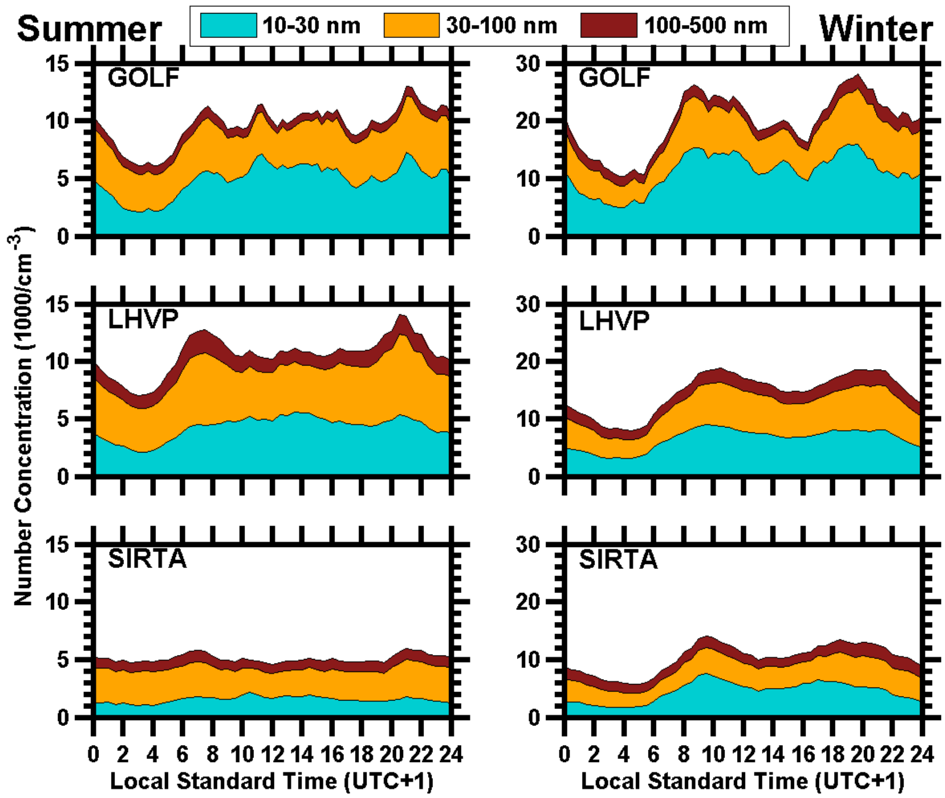

Fig. 7. Number concentration diurnal profiles of summer (left) and winter (right) campaigns for size ranges from 10 to 30 nm, 30 to 100 nm, and 100 to 500 nm, respectively. Different scales are used for each season.

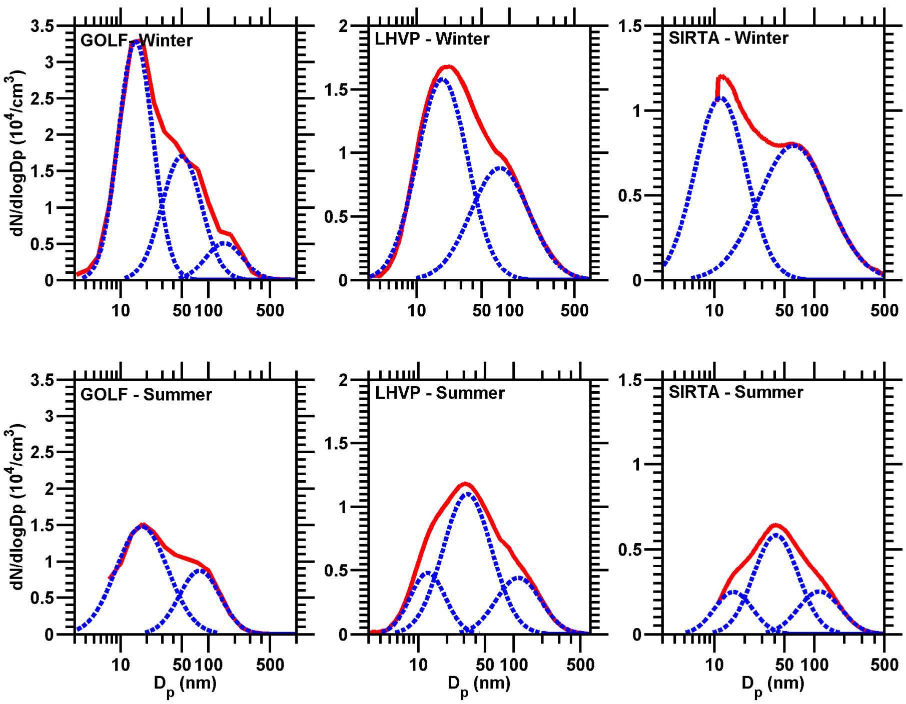

Fig. 8. Campaign average particle number distributions for winter (top) and summer (bottom) for the three ground sites based on measurements of EAS at GOLF, DMPS at LHVP and SMPS at SIRTA. Each average size distribution (solid red line) is deconvoluted to lognormal modes (dashed blue lines). Note the different scaling of the y-axes between sites.

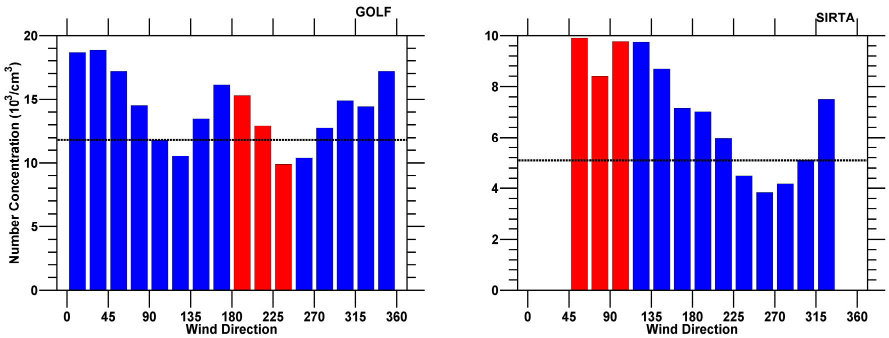

Fig. 9. Number concentrations measured at the two satellite sites during summer with respect to wind direction / air mass transport direction measured at the respective site. The angles which indicate that the air mass traveled through the city center prior to reaching the site are depicted in red. The horizontal dashed black line corresponds to the campaign average for each site. Periods with wind speed below 1 m s^{-1} were omitted from the analysis.

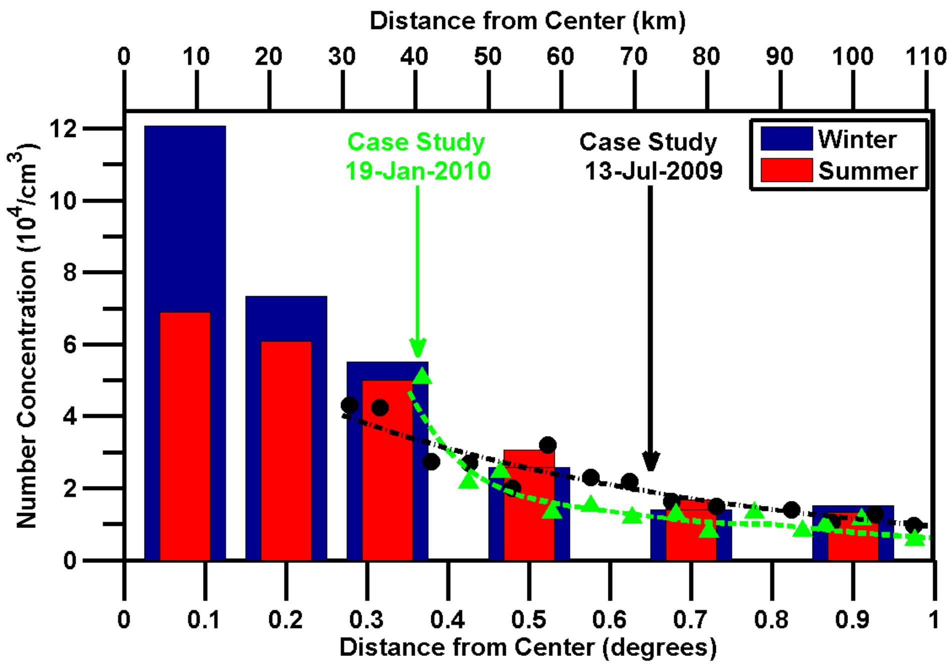

Fig. 10. Average number concentration ($N_{2.5}$) with respect to distance from the city center measured by the mobile platforms during summer (red) and winter (blue). During both campaigns an exponential decrease of the number concentration with respect to distance was observed. The number concentration measured in an axial measurement on a case study day is also depicted in the graph for summer (black dots) and winter (green triangles).

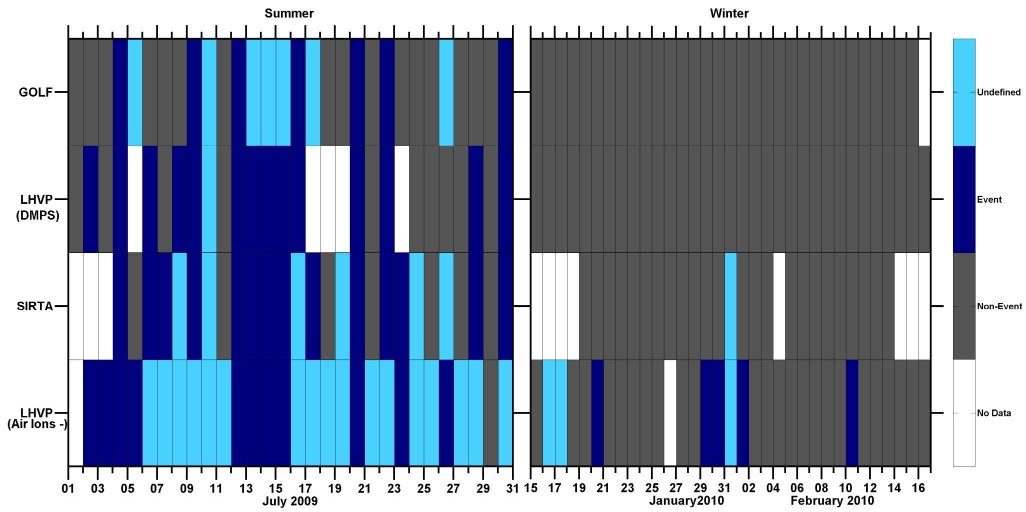

Fig. 11. Nucleation analysis results during summer and winter for all ground sites. Events, non-events, undefined and lack of data are depicted in blue, grey, light blue and white, respectively.

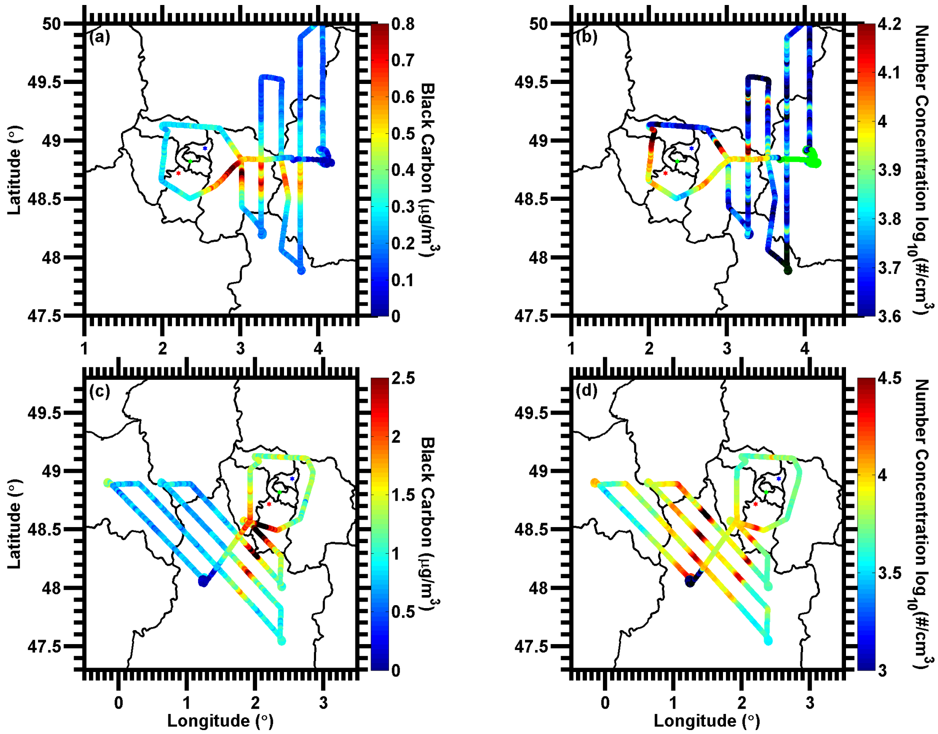

Fig. 12. Flight trajectories for 9th (a, b) and 1st (c, d) July 2009, color coded for black carbon and number concentrations (N_{10}), respectively. Black carbon concentrations are used as tracers of the Paris plume (a, c); its direction relative to the city center indicates wind direction. Red, green and black dots within the figure correspond to the locations of SIRTA, LHVP and GOLF, respectively. Increased number concentrations were observed outside of the plume. During July 9 (b) the area where the number concentration increased was located upwind of the city center and NPF was identified at all ground sites. During July 1 (d) the particle number increase was observed along the plume. The number and black carbon concentration corresponding to c and d are also shown with respect to time in Suppl. Fig. 3.